PERFORMANCE OF SHORT ANCHORS INSIDE THE FAILURE WEDGE

A THESIS SUBMITTED TO
THE GRADUATE SCHOOL OF NATURAL AND APPLIED SCIENCES
OF
MIDDLE EAST TECHNICAL UNIVERSITY

BY

BERK DEMİR

IN PARTIAL FULFILLMENT OF THE REQUIREMENTS
FOR
THE DEGREE OF MASTER OF SCIENCE
IN
CIVIL ENGINEERING

SEPTEMBER 2019

Approval of the thesis:

PERFORMANCE OF SHORT ANCHORS INSIDE THE FAILURE WEDGE

submitted by **BERK DEMİR** in partial fulfillment of the requirements for the degree of **Master of Science in Civil Engineering Department, Middle East Technical University** by,

Prof. Dr. Halil Kalıpçılar
Dean, Graduate School of **Natural and Applied Sciences** _____

Prof. Dr. Ahmet Türer
Head of Department, **Civil Engineering** _____

Assist. Prof. Dr. Onur Pekcan
Supervisor, **Civil Engineering, METU** _____

Examining Committee Members:

Assist. Prof. Dr. Nabi Kartal Toker
Civil Engineering, METU _____

Assist. Prof. Dr. Onur Pekcan
Civil Engineering, METU _____

Prof. Dr. Bahadır Sadık Bakır
Civil Engineering, METU _____

Assist. Prof. Dr. Nejan Huvaj Sarıhan
Civil Engineering, METU _____

Assist. Prof. Dr. Ebru Akış
Civil Engineering, Atılım University _____

Date: 20.09.2019

I hereby declare that all information in this document has been obtained and presented in accordance with academic rules and ethical conduct. I also declare that, as required by these rules and conduct, I have fully cited and referenced all material and results that are not original to this work.

Name, Surname: Berk DEMİR

Signature:

ABSTRACT

PERFORMANCE OF SHORT ANCHORS INSIDE THE FAILURE WEDGE

DEMİR, Berk
Master of Science, Civil Engineering
Supervisor: Assist. Prof. Dr. Onur Pekcan

September 2019, 92 pages

The most widely accepted rule of thumb for anchor design is that bonded length of the ground anchors should be placed outside the failure wedge in order to increase resistance against overall stability. Moreover, failure wedge is defined as "no load zone." This study investigates the performance of anchors inside and outside of the failure wedge by parametric studies performed through finite element analyses using Plaxis 2D and 3D. An anchored retaining wall with short and long anchors is compared with only long anchors in different arrangements. Seven long anchors (base model) are compared with additional seven short and long anchors to investigate the effect of anchor length on the retaining wall behavior. Also, different cases such as equal anchor quantity, equal addition to seven long anchors model and constant horizontal spacing are investigated. An efficiency term is defined to effectively compare these cases. Analyses have shown that anchors inside the failure wedge do not reduce factor of safety against overall stability, but decrease the lateral deformation of the retaining system. In fact, short anchors' performance on decreasing lateral deformations is found to be better than long anchors for practical comparisons. Results are compared with 3D analyses, different finite element packages and soil models. Also, importance of modelling anchors using elasto-plastic models are emphasized. Lastly, anchor

model and associativity analyses have been performed to reflect the effect of various elements on the failure surface.

Keywords: Deep Excavation, Finite Element Method, Anchor, Retaining Wall

ÖZ

KAYMA KAMASI İÇERİSİNDEKİ KISA ANKRAJLARIN PERFORMANSI

DEMİR, Berk
Yüksek Lisans, İnşaat Mühendisliği
Tez Danışmanı: Dr. Öğr. Üyesi Onur Pekcan

Eylül 2019, 92 sayfa

Ankraj tasarımının en yaygın kabul edilen temel kuralı ankraj kök boylarının, genel stabilite yenilmesine karşı dayanımı arttırmak için kayma kamasının dışına çıkarılmasıdır. Bunun yanında, kayma kamasının içerisi "yük almayan bölge" olarak tanımlanmaktadır. Bu çalışma, kayma kaması içinde ve dışındaki ankraj davranışlarını Plaxis 2D ve 3D sonlu elemanlar yöntemleri yardımıyla parametrik olarak incelemektedir. Sadece uzun ankrajlar içeren bir ankrajlı iksa duvarı, kısa ve uzun ankrajlar içeren iksalar ile farklı durumlarda karşılaştırılmıştır. Yedi uzun ankrajlı modele ek olarak yapılan yedi kısa ve uzun ankrajla karşılaştırılarak ankraj boyunun iksa davranışına etkisi araştırılmıştır. Ayrıca, eşit ankraj miktarı, 7L modeline eşit ekleme ve eşit yatay aralık gibi farklı durumlar incelenmiştir. Kayma kaması içinde kalan ankrajlar genel stabiliteye karşı güvenlik sayısını azaltmamakla birlikte, yatay deplasmanları azaltmaktadırlar. Hatta, kısa ankrajların yatay deplasmanları azaltmadaki performansının uzun ankrajlara göre daha iyi olduğu tespit edilmiştir. Sonuçlar 3D analizler, farklı sonlu elemanlar paketleri ve zemin modelleri ile karşılaştırılmıştır. Ayrıca, ankrajların elasto-plastik modellenmesinin önemi vurgulanmıştır. Son olarak, ankraj modeli ve akma modeli analizleri yapılarak çeşitli etmenlerin kayma düzlemine etkileri incelenmiştir.

Anahtar Kelimeler: Derin Kazı, Sonlu Elemanlar Metodu, Ankraj, İksa

Oğuz Atay’a.

ACKNOWLEDGEMENTS

I would like to express my sincerest gratitude to Asst. Prof. Dr. Onur Pekcan for unlimited patience and academical guidance for me since my internship as an undergraduate student. I wouldn't complete my thesis without his understanding.

I am grateful to Asst. Prof. Dr. Nabi Kartal Toker for valuable comments and giving me important insights.

I am thankful to Asst. Prof. Dr. Nejan Huvaj Sarıhan for introducing me to geotechnical community by taking me with her to my first geotechnical symposium in Adana.

I would like to thank Görkem Eken, my dear friend, for helping me since my very first days in university. Without his support, I wouldn't even finish my BS.

My mother and father, Seniye and Hayrettin Demir have worked and saved for their entire lives to provide for us. Their dedication to raise us as well-educated people has brought me to where I am.

Lastly, I am very thankful to Pınar Akdoğan, for her continuous support and encouragement. She always kept me in the mood to study and never let me to fall down.

TABLE OF CONTENTS

LIST OF TABLES

TABLES

LIST OF FIGURES

FIGURES

LIST OF ABBREVIATIONS

ABBREVIATIONS

2D	Two-dimensional
3D	Three-dimensional
ASTM	American Society for Testing and Materials
BS	British Standards
C	Capped Model (Elasto-plastic)
CPT	Cone Penetration Test
CPU	Cental Processing Unit
FELA	Finite Element Limit Analyses
FEM	Finite Element Method
FHWA	Federal Highway Administration
FS	Factor of Safety
HS	Hardening Soil
HSSmall	Hardening Soil Small
LEM	Limit Equilibrium Method
MC	Mohr-Coulomb
NC	No Cap Model (Elastic)
PI	Plasticity Index
PTI	Post Tensioning Institute
SPT	Standard Penetration Test

LIST OF SYMBOLS

SYMBOLS

c'	Effective cohesion
c_c	Compression index
c_s	Swelling index
c_u	Undrained shear strength
E	Modulus of elasticity
E_0, E_{max}	Maximum Modulus of Elasticity at zero strain.
E_{50}	Triaxial secant stiffness
E_{oed}	Oedometer loading stiffness
E_u	Undrained modulus of elasticity
E_{ur}	Unloading/reloading modulus
FS	Factor of Safety
g	Plastic potential function
G	Shear Modulus
G_{max}	Maximum Shear Modulus
G_{ur}	Unloading/reloading shear modulus
K_0	Coefficient of lateral earth pressure at rest
m	Amount of stress dependency
p_{ref}	Reference stress level
R_f	Strain level at failure
v	Poisson ratio
v_s	Shear wave velocity
v_{ur}	Unloading/reloading poisson ratio
y	Yield function
γ	Shear strain
$\gamma_{0.7}$	Threshold strain

$\delta\gamma_m$	Shear strain change
$\delta\varepsilon_v$	Volume change
λ	Failure angle
σ_1'	Effective vertical stress
σ_3'	Effective confining pressure
η	Efficiency coefficient
τ	Shear strength
τ_f	Shear stress on the rupture surface
ϕ'	Effective friction angle
ϕ_{cv}	Critical state friction angle
ϕ_m	Mobilized friction angle
ψ	Dilatancy angle
ψ_m	Mobilized dilatancy angle

CHAPTER 1

INTRODUCTION

1.1. Research Background

Retaining walls have been integral part of high-rise structures to provide deeper basements. During their construction, different types of lateral supports are used to provide stability of the foundation excavation. Among those, prestressed ground anchors are one of the most widely used lateral supports not only to provide resistance against global stability failure and but also to limit the displacement of the walls.

Even though it is one of the oldest topics in geotechnical engineering field, the design of a retaining wall still contains complications and arguable issues. For proper design purposes, some rules of thumb have been developed throughout the decades, mostly based on the earth pressure theories and observations from actual field experiences.

Considering the design of prestressed ground anchors, the most widely accepted rule of thumb is that the bond length should be placed outside the failure wedge to increase resistance against overall stability failure. FHWA-IF-99-015 (Sabatini, Pass, & Bachus, 1999) defines a “no load zone” which is the zone between potential active failure surface and retaining wall. Using this analogy, FHWA suggest that anchors should reach beyond the failure surface at least 1.5m or 20% of the height of the excavation, whichever is highest. Eurocode 7 (British Standards Institution, 2004) leaves the decision on failure surface to designer and states that anchor bond length should be “sufficiently distant” from retained volume in order to not “adversely affect” the stability. Canadian Foundation Engineering Manual (2006) states anchors should reach outside of a potential failure plane and “are not placed within a potentially deforming soil mass.” BS 8081 (British Standards Institution, 2015) requires placing anchors’ bonded lengths beyond “any potential failure surface.”

Ou (2006) clearly states that anchors should be placed outside of the potential active failure surface by at least 2 meters to maintain overall stability and also presents mostly used failure surfaces which include FHWA failure surface and other surfaces that start from an assumed hinge point between the excavation depth and toe of the wall. For rigid walls which do not fail before the global soil failure, failure surface that originates from the toe of the wall provides most accurate results. For flexible walls, FHWA failure surface is more correct due to developed hinge at the flexible wall. Clayton (2014) suggests an overall stability analysis would ensure that anchor forces are transmitted outside of the failure wedge which means unbonded lengths of anchors are adequate. Anderson et. al. (1983) defines the Kranz and Broms methods which deals with force equilibrium of active wedge and states that an additional requirement to these methods is "no part of fixed anchorage length should be located within the active earth pressure zone." Briaud and Lim (1999) note that as long as fixed lengths of anchors are outside of the potential failure zone, length of anchors do not have significant effect on bending moment and axial loads. The terms and surfaces mentioned above are shown in the *Figure 1.1*:

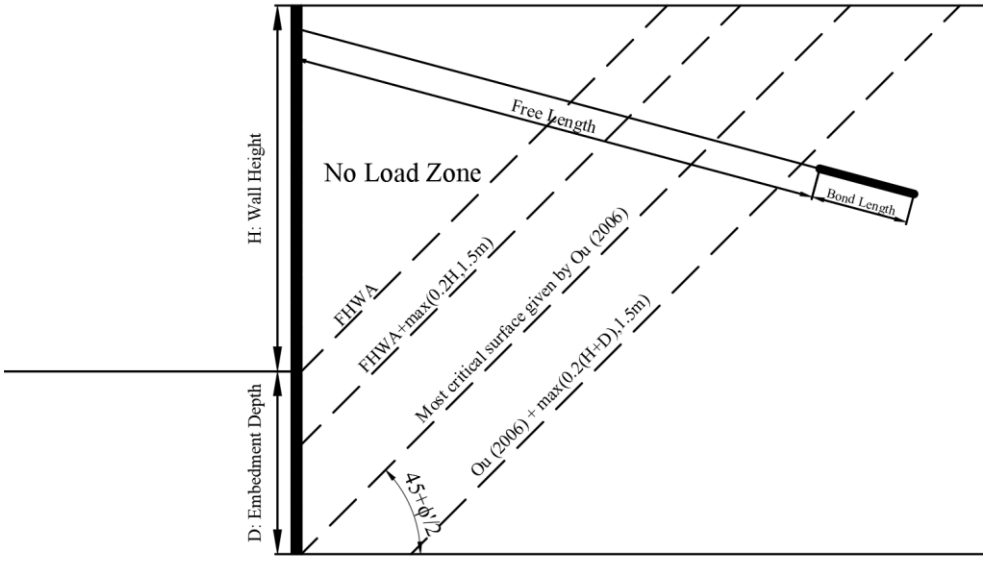

Figure 1.1. Failure Surfaces in Literature and Nomenclature

Considering the above literature work, it is quite apparent that the decision made for the length of the anchors is quite important in the design where the geometry of the failure wedge dominates their behavior. In this sense, short anchors are defined as the anchors with bond lengths inside the failure wedge, while long anchors' bond lengths are outside the failure wedge. Although the literature works quite apparently defined the design rules, the engineering principles of design for short anchors remained in the shadow and left questionable for future studies.

1.2. Research Objectives

With the above perspective, in order to bring some insight to the problems related with short anchors, such as defining their behavior in terms of both displacement and factor of safety, this study aims to investigate the performance of short anchors compared to long anchors under different arrangements such as equal horizontal spacing, equal addition to base model and equal quantity. The claim of this work is that while the long anchors provide resistance against overall stability failure, short anchors may be useful to reduce lateral displacement and forces on retaining walls. With this, the eventual aim of this study is to re-visit the well accepted rule of thumb in anchor design.

1.3. Scope of the Study

This study deals with extensive comparison of short and long anchors based on their effects on retaining wall systems. Effects of short anchors are investigated based on the displacement criterion and safety factor against overall stability and economy. In addition, the effect of anchor modeling and associativity are discussed since these factors may affect overall stability behavior significantly.

1.4. Research Methodology

To quantify the performance of short and long anchors, engineering analyses based on finite element method (FEM) are mainly used. FEM implemented in the analyses are formed for both 2 dimensional plain strain and 3 dimensional cases. For 2D analyses, Plaxis 2D software package is used to perform finite element analyses, while for 3D ones, Plaxis 3D (v2016.2) is used. In addition to these, another finite element based limit analysis software, named Optum G2, is used for both comparison and validation purposes.

Currently there are various approaches available to be used for modelling the interaction between anchors and soil and stability of retaining structures. Considering many of them, FEM can provide a robust approach to simulate the stability provided by anchors on the failure wedge. Although there are other software packages to analyze anchored retaining walls, these packages use apparent earth pressure theories to design retaining wall systems. The results obtained from these packages are somehow irrelevant to this study as they are developed based on the same rule of thumb this study questions. Therefore, the potential investigations made with such software are kept out of the scope of this study.

1.5. Organization of the Thesis

The next chapter presents the literature review on the soil behavior and modeling related to retaining walls and prestressed anchors, and provide the related work for numerical analysis methods developed so far. Chapter 3 presents the results of the analyses to investigate effects of anchor modeling. The performance of short anchors and effect of association on the failure surface are also discussed in this chapter. Finally, Chapter 4 presents the summary, conclusion and future works.

CHAPTER 2

LITERATURE REVIEW

Due to increasing need of space in densely populated cities, basement excavations to provide parking space or utility storage are becoming deeper. To avoid any damage to nearby buildings and overall stability problems, anchored retaining walls have been used to support these excavations. This chapter provides literature review of studies related to design of anchored retaining walls and its aspects.

2.1. Soil Behavior and Modelling

To design a civil engineering structure, behavior of material used in the construction should be known. However, unlike most commonly used materials in civil engineering industry such as concrete or steel, soil is not homogenous nor manufactured. Due to complex structure of soil fabric, understanding the soil behavior has always been most challenging task of geotechnical engineering.

This chapter summarizes some of the theoretical and experimental studies performed on this area. Special attention is given to behavior of soils in retaining systems and soil modelling in finite element method.

Brinkgreve (2005) presented an excellent summary of all factors that affect the soil behavior.

Table 2.1. Brinkgreve's (2005) Summary of Factors Affecting Soil Behavior

Aspect	Definition
Influence of water	Mechanical behavior of soil is dominated by effective stress. To calculate effective stress, pore pressures are important.
Soil stiffness	Soil stiffness is not constant and depends on many factors.
Stress level	Confining stress ↑ Stiffness ↑
Stress path	Stiffness during unloading > Stiffness during primary loading
Strain level	Strains ↓ Stiffness ↑
Time (duration)	Time ↓ Stiffness ↑
Density	Density ↑ Stiffness ↑
Permeability	Undrained stiffness > Drained or unsaturated stiffness
Over-Consolidation	Over-consolidated stiffness > Normally consolidated stiffness
Direction	Stiffness anisotropy is important factor in some soils.
Irreversible Deformations	Difference between elastic and plastic deformations.
Strength of Soils	Strength of soils too, depends on many factors.
Stress Level	Confining stress ↑ Strength ↑
Loading Speed	Loading speed ↑ Strength ↑
Time (duration)	Strength may increase (i.e. cementation) or decrease (degradation) with time.
Density	Density ↑ Strength ↑ However, dense soils may show softening behavior after peak strength.
Undrained behavior	Undrained shear strength should be considered.
Over-Consolidation	Higher shear strength followed by softening.
Direction	Strength anisotropy.
Time Dependency	Consolidation, creep, relaxation, swelling.
Compaction & Dilatancy	Upon shearing, loose soil will compressed, dense soil will dilate. Clays usually do not show any dilatancy behavior.
Memory of Pre-Consolidation	Over-consolidated or Normally consolidated behavior distinction. Reconstituted soils do not have memory.

2.1.1. Strength of Soils

Strength properties of the soils can be modelled using variety of assumptions. Failure criterion is one of these assumptions. Mohr-Coulomb failure criterion is one of the most commonly used one while other criteria like Tresca, Von Mises and Drucker-Prager are still valid. (Ou, 2006)

Mohr-Coulomb failure criterion is developed based on the works of Coulomb (1773) on thrust acting on retaining wall. Mohr-Coulomb failure criterion is represented by hexagonal cone in 3D space of principal stresses (*Figure 2.1*). Drucker-Prager criterion is developed as an improvement to Mohr-Coulomb where hexagonal cone is replaced with circular cone to avoid numerical implementation errors. (Potts, Axelsson, Grande, Schweiger, & Long, 2002) However, Drucker-Prager criterion's fit to behavior of soil is found to be more erroneous than Mohr-Coulomb. (Britto & Gunn, 1987) Yield surfaces that have hexagonal bases with rounded corners, such as Von Mises, are also used in researches. *Figure 2.1* shows the comparison of both yield surfaces in 3D stress space.

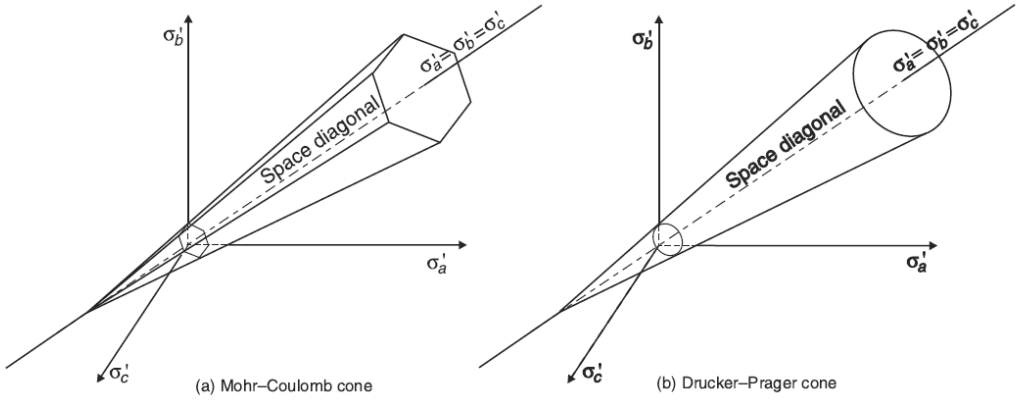

Figure 2.1. Mohr-Coulomb and Drucker-Prager Failure Surfaces Comparison (Potts et al., 2002)

Mohr-Coulomb failure criterion is defined by effective cohesion, c' and effective friction angle, ϕ' based on the formula given below in effective stress form:

$$\tau = c' + \sigma' \cdot tan(\phi') \quad (1)$$

Mohr-Coulomb failure criterion is originally based on associated flow rule. Modified Mohr Coulomb model which is used in most of finite element codes include additional plastic potential function, g. In case of g≠y where y is yield function, non-associated flow rule is governing the equation.

For perfectly plastic soils where yield potential is same with plastic flow potential, associated flow rule governs. Associated flow means that friction angle of soil is equal to dilatancy angle, ψ. For ϕ≠ψ cases, non-associated flow rule applies where plastic increment vectors are not normal to yield surface. Dilatancy angle is defined in terms of volume change ($\delta\varepsilon_v$) during shearing of soil ($\delta\gamma_m$) and can be formulized as below. (Parry, 2014)

$$sin(\psi) = -\frac{\delta\varepsilon_v}{\delta\gamma_m} \quad (2)$$

Detailed information on the effect of dilatancy to behavior of soil will be presented in Chapter 2.2.1.

2.1.2. Soil Models

After popularization of high CPU power computers, finite element methods have been the most popular tool to model soil behavior and geotechnical structures. To model a soil, strength and stiffness properties of each mesh element in the soil should be characterized by set of equations which are commonly called soil constitutive models. Soil models have been developed based on theoretical and experimental results and validated using different case studies.

Constitutive models used throughout the study are described here. Although soil models are common to all FEM codes, in case of any difference, Plaxis Finite Element Code have been used as main reference.

- **Mohr-Coulomb Model – MC:**

Mohr-Coulomb model is first order approximation of soil behavior using 5 input parameters. Soil stiffness is modelled using E and v, which are modulus of elasticity and Poisson's ratio respectively. Strength characteristics are modelled using c, ϕ and ψ. Modulus of elasticity does not depend on stress, however, linear change with depth can be imposed. (Plaxis BV, 2017a) If cohesion value is selected as undrained cohesion, Mohr-Coulomb failure surface is same with Tresca failure surface.

Mohr-Coulomb model is linear elastic perfectly plastic type of model. Therefore, after stresses reach hexagonal yield surface, strains become plastic and continue to increase without increase in stress.

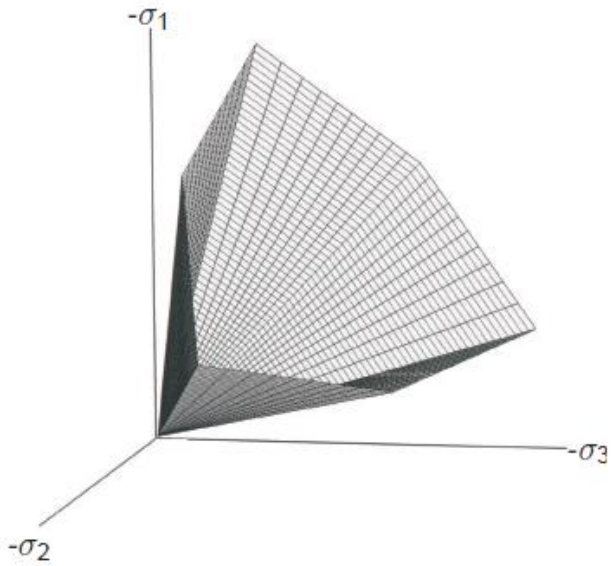

Figure 2.2. Mohr-Coulomb Model Yield Surface (Plaxis BV, 2017a)

Plaxis Material Manual (2017a) recommends using E_{ur} for E to model unloading problems such as tunneling and excavations. Since Mohr-Coulomb stiffness definition does not depend on stress path or stress level, using appropriate elastic modulus based on stress and strain level of given problem is necessary.

- **Hardening Soil Model – HS:**

Schanz et. al. (1999) formulated hardening soil model based on Mohr-Coulomb failure criterion using theory of plasticity and Duncan & Chang's (1970) hyperbolic model. Elasto-plastic Hardening Soil Model's yield surface, unlike MC, can expand with increasing plastic strain. Stiffness is modelled using three distinct moduli: Triaxial loading stiffness, E_{50}; Triaxial unloading stiffness, E_{ur}; Oedometer loading stiffness, E_{oed}. Other input parameters required by Hardening Soil Model are c', ϕ', p^{ref} (reference stress level at which elastic moduli are calculated, usually taken as 100 kPa), m (power of stress dependency), v_{ur} (poisson ratio for unloading/reloading), ψ, K_0 and R_f. (strain level at failure, usually taken as 0.9.)

E_{50} modulus is confining stress dependent, therefore can represent primary loading behavior of the soil better than E_1 which is experimentally harder to measure. (Schanz et al., 1999)

Hardening Soil Model implements hyperbolic model which is developed by Duncan & Chang (1970) formula which relates E_{50} to confining stress. (Plaxis BV, 2017a; Schanz et al., 1999) Similar formula is used with unloading and oedometric stiffness too.

$$E_{50} = E_{50}^{ref} \left(\frac{c \cos \phi - \sigma_3' \sin \phi}{c \cos \phi + p^{ref} \sin \phi} \right)^m \quad (3)$$

In the formula above, m is amount of stress dependency, σ_3 is effective confining pressure in triaxial test and p_{ref} is reference stress. Recommended m for soft clays is 1.0 due to logarithmic stress dependency. (Schanz et al., 1999) For sands, recommended m value is between 0.5 and 1.0. (Plaxis BV, 2017a)

E_{ur}, triaxial unloading stiffness or reloading stiffness, can be calculated using swelling index which can be obtained from an oedometer test. Plaxis also allows user to input c_c and c_s, which are compression and swelling index respectively, to calculate stiffness modulus. Also, a simple relationship between E_{50} and E_{ur} is recommended by some studies. Poulos (2017) states E_{ur} is usually 3 to 5 times of E_{50}. Hong Kong manual on Pile Design and Construction (1996) recommends ratio of 2 to 3 times. Kempfert & Gebreselassie (2006) states E_{ur} is usually around 5 to 7 times of E_{50}, but recommends using $3E_{50}$ with the absence of test results. Obrzud (2010) recommends assuming E_{ur} equal to 3 to 10 times of E_{50} by relating with the standard c_c/c_s ratio observed in oedometer tests. Optum G2 Material Manual (2018a) recommends assuming 2 to 5 for E_{ur}/E_{50} ratio while Plaxis (2017a) recommends 3. Kulhawy & Mayne (1990) presents correlation of c_c and c_{ur} with PI. Based on the recommended best fit, c_c/c_{ur} which is also equal to E_{ur}/E_{50} is 5.

HS Model, based on the experimental evidence, adopts zero dilation below mobilization of friction angle to 0.75 of peak friction angle. Then, mobilized friction angle is calculated using the formula below which is adapted from Rowe (1962). Critical state angle is calculated using the maximum dilatancy angle and friction angle. Critical state is not stress-dependent and constant throughout all strain ranges.

$$\sin\psi_m = \max\left(\frac{\sin\phi_m - \sin\phi_{cv}}{1 - \sin\phi_m \sin\phi_{cv}}, 0\right) \quad (4)$$

Most important limitation of HS Model is assumption of same stiffness modulus in all strain ranges. Although the stiffness modulus changes with different stresses as given in Eq. 3, strain-dependent reduction is not adopted in this soil model. Also, yield surface expands by the same amount in all direction, therefore model is completely isotropic which is not always the case for soils.

Advantages of HS Model over MC Model are presented by Teo & Wong (2012) and are listed below:

- Nonlinear behavior before failure.

- Stress-dependent stiffness.
- Unloading-reloading behavior.
- Better 1D compression fit.
- MC produce incorrect response under certain stress paths.
- MC under-estimates horizontal stress under certain stress paths.
- MC is sensitive to poisson ratio.

- **Hardening Soil Model with Small Strain Stiffness - HSSmall**

In the preface of dissertation by Thomas Benz (2007), Vermeer states that using HSSmall model, depth of influence (i.e. limit depth or active compression zone) can be determined without limiting the model size. This advanced behavior is provided by HSSmall model's advanced strain-based stiffness modelling.

Stiffness of soil is strictly dependent on strain level. This behavior has been shown in literature by various researches using degradation (G/Gmax) vs. strain curves, such as Seed & Idriss (1970). Benz (2007) reproduced the curve by Atkinson & Salfors (1991) and Mair (1993) that introduce general strain ranges in geotechnical applications.

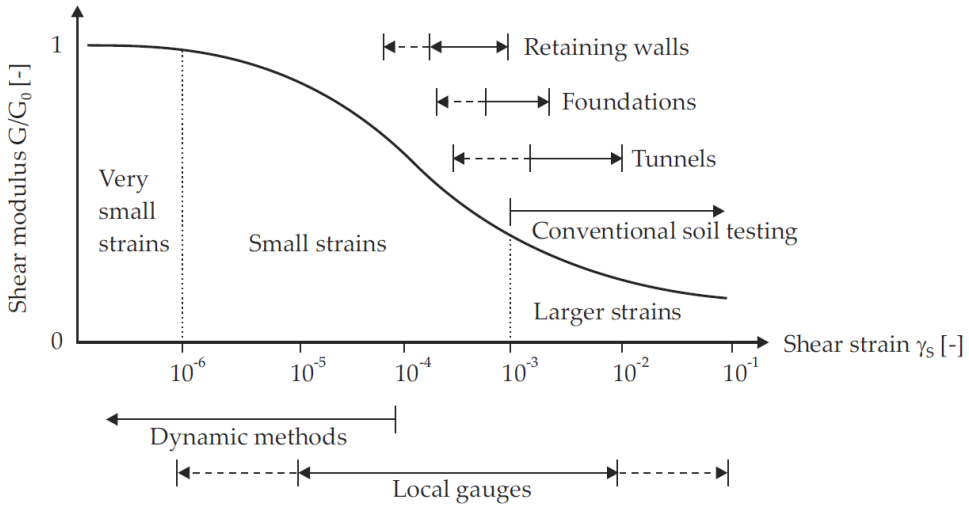

Figure 2.3. G/Gmax vs. Strain Curve with General Ranges (Benz, 2007)

Figure 2.3 shows that stiffness of soil is strain dependent and cannot be assumed equal for all strain ranges. To improve HS Model, Benz (2007) included strain dependence to stiffness using Hardin & Drnevich (1972) modulus reduction curve with threshold value defined by Santos & Correia (2001) as 70%.

$$\frac{G}{G_{max}} = \frac{1}{1 + 0.385 \left|\frac{\gamma}{\gamma_{0.7}}\right|} \tag{5}$$

In the formula given above, G_{max} is the maximum shear modulus, G is the shear modulus at given shear strain, γ is the current strain and $\gamma_{0.7}$ is the shear strain at G/G_{max} equals 70%.

Shear strain at $G/G_{max} = 0.7$ can be determined using variety of G/G_{max} curves that can be found in literature such as Vucetic & Dobry (1991) curve.

To determine G_{max}, there are variety of ways which includes analytical and empirical correlations. Since G_{max} is shear modulus corresponding to minimum shear strain (around 10^{-6}) calculated values using geophysical methods are valid for this range.

$$G_{max} = \rho \, V_s^2 \; (kPa) \tag{6}$$

Shear wave velocity can be computed directly from the geophysical field and laboratory test or using the correlations based on SPT and CPT. G_{max} can also be computed using correlation presented by Alpan (1970) in the form of E_0 / E_{ur} vs. E_{ur} and reproduced by Benz (2009) using additional data available in the literature. The following equation is fitted to Alpan's (1970) chart with R^2 value 0.98.

$$\frac{E_0}{E_{ur}} = 24.467 \cdot E_{ur}^{-0.448} \tag{7}$$

Since required input for HSSmall model is G_{max}, presenting this formula with G_{max}/E_{ur} will be more convenient. Using the elasticity theory, $E_0 = 2 \cdot (1 + \nu) \cdot G_0$ and assuming $\nu = 0.2$ for elastic range, G_{max}/E_{ur} ratio of Alpan (1970) can be defined as:

$$\frac{G_{max}}{E_{ur}} = 10.194 \cdot E_{ur}^{-0.448} \quad (8)$$

Brinkgreve et. al. (2007) states that, for soft soils G_{max}/G_{ur} ratio around 10, while for stiffer soils this ratio may decrease to 2.5. If these ratios are converted to G_{max}/E_{ur} using previous assumptions, ratios will be 4 and 1 respectively. Plaxis also limits G_{max}/G_{ur} ratio at 20. (Plaxis BV, 2017a)

To avoid very small stiffness values at higher strains, Benz (2007) introduced a cut-off value based on the HS Model parameter E_{ur}. Minimum shear modulus of the soil is limited to G_{ur} which is calculated using elasticity theory based on E_{ur} and ν_{ur}. Cut-off shear strain is calculated as:

$$\gamma_c = \frac{\gamma_{0.7}}{0.3805}\left(\sqrt{\frac{G_0}{G_{ur}}} - 1\right) \quad (9)$$

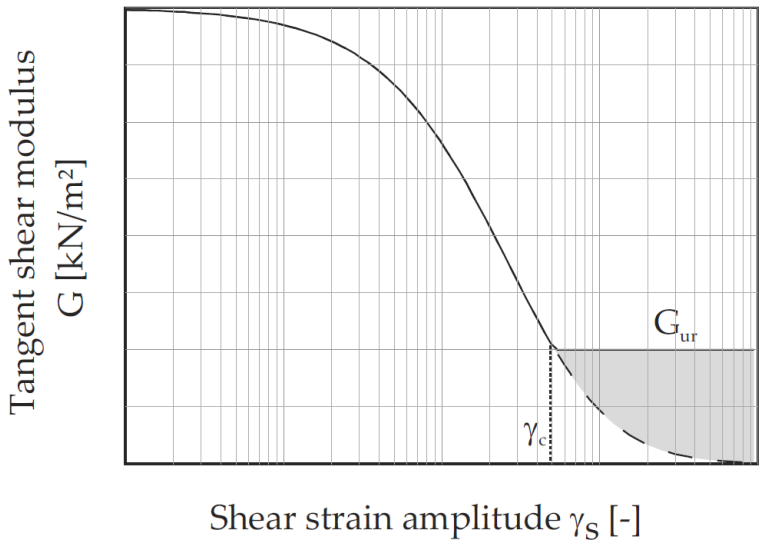

Figure 2.4. Cut-off in Stiffness Degradation Curve (Benz et al., 2009)

2.2. Retaining Walls

Design of retaining walls, before the implementation of finite element methods in geotechnical engineering, have been mostly performed using earth pressure theories by Rankine (1857) and Coulomb (1773).

Rankine earth pressure theory is based on plastic equilibrium. Soil behind the wall may fail due to decrease in horizontal pressure, i.e. active case, therefore radius of Mohr circle increases. Similarly, passive failure occurs when horizontal pressure applied on the retaining wall increases. Failure surface is assumed to be located at $45 + \phi'/2$. Lateral pressures are calculated using coefficient of lateral pressure at active, passive or at-rest (no horizontal deformation) states. Due to change of major axis by 90° during passive loading (since σ_1 is horizontal), required strain to mobilize passive failure is approximately four times the required strain to mobilize active conditions.(NAVFAC, 1986)

One important assumption of Rankine theory is that soils inside the failure wedge are assumed to be at failure. Consequences of this assumption will be detailed later, but simply Rankine theory assumes “infinite failure surfaces.” (Ou, 2006)

Coulomb earth pressure theory considers the weight of the retained soil behind retaining wall to establish an equilibrium. Calculation of earth pressure coefficients includes wall and ground surface angles.

Details of both methods can be found in soil mechanics textbooks. Limitations of these theories have been discussed by Ou (2006). Assumption of planar surface, frictionless contact between wall and soil, irregular site conditions, different passive earth pressure behavior in field, applicability of Coulomb theory to cohesionless soil only are only few of them.

Lateral supports have been designed to reduce to deformations, structural forces and possibility of overall shear failure. Before finite element method, determination of

loads on the supports have been based on empirical load envelopes such as given by Terzaghi, Peck & Mesri. (1996)

Beam on elastic foundation method have been also used extensively to predict the behavior of retaining systems using springs. Especially, structural engineers continue to use this method with structural design software packages that implement spring-based approaches. However, determining the soil behavior using linear springs or perfectly plastic springs is not easy, therefore should be treated carefully.

2.2.1. Progressive Failure of Retaining Walls

Studies on retaining walls, due to complex nature of the topic, have become diversified on number of areas. Introductory information on limited number of topics will be presented here. Detailed information can be found in number of books on these topics. (Kempfert & Gebreselassie, 2006; Ou, 2006; Puller, 2003)

Global stability failure is the most important failure type for retaining walls due to catastrophic collapse. The failure gradually progresses along the failure surface rather than happening simultaneously across the failure surface. As Poulos et. al. (2001) states Rankine and Coulomb theories assume that all soils along (or inside for Rankine case) the failure surface fail at the same time. A number of model tests have shown that this assumption is not true. Failure occurs at individual soil elements through a surface (based on stress or velocity characteristics). Each element, independent of the other, forms an infinitesimal surface. If this surface connects to each other and free boundary where movements are not restrained, this bundle of failed elements are named as failure surface. If boundary conditions are restrained, failure will not occur. For example, soil cannot fail in oedometric conditions due to lateral restrains, but only settle.

Most important study on this area is performed by Rowe and Peaker (1965). Based on their model tests, they proposed a block analogy. Blocks are connected to each other by series of springs and rests on the failure surface at the bottom. Clayton et. al. (2014) presents this analogy graphically. Shear stress vs. displacement graph in *Figure 2.5*-b

shows that while soils just behind the wall reaches critical state, soil far from the wall is at the elastic phase.

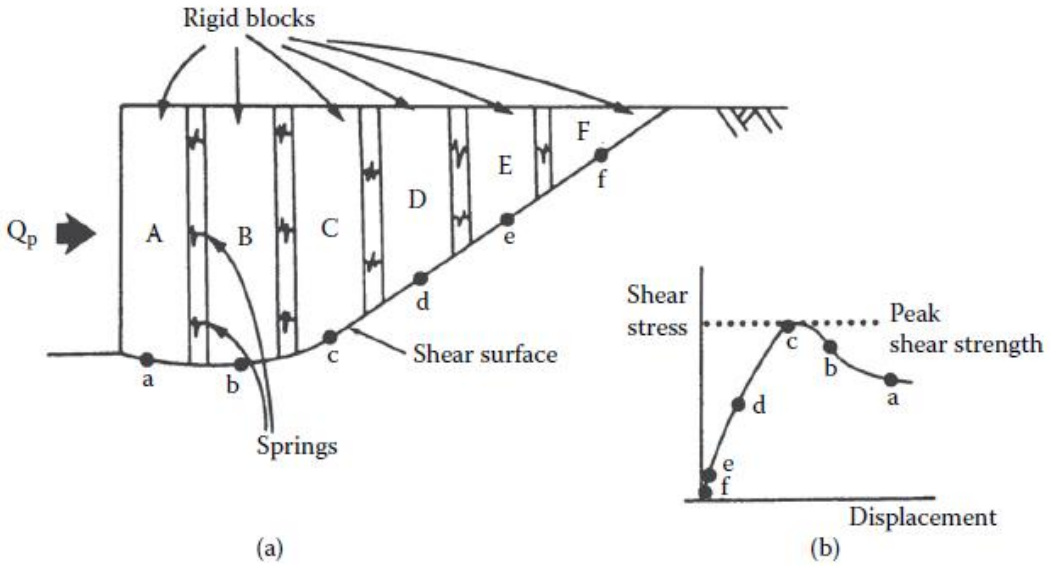

Figure 2.5. Rigid Block Analogy (Clayton et al., 2014; Rowe & Peaker, 1965)

Rigid blocks connected with springs represents a different behavior then Rankine assumptions as can be seen. Soils inside the blocks do not fail, but only soils at the shear surface fail. Therefore, it can be concluded that, with the notation given in *Figure 2.5* point 'a' fails, not block 'A'. Although Coulomb method assumes rigid soil block, assumption of simultaneous failure along the failure surface is not a valid simplification of soil behavior.

A similar example is given by Duncan et. al. (2014) for over-consolidated clay with strain softening behavior with respect to time.

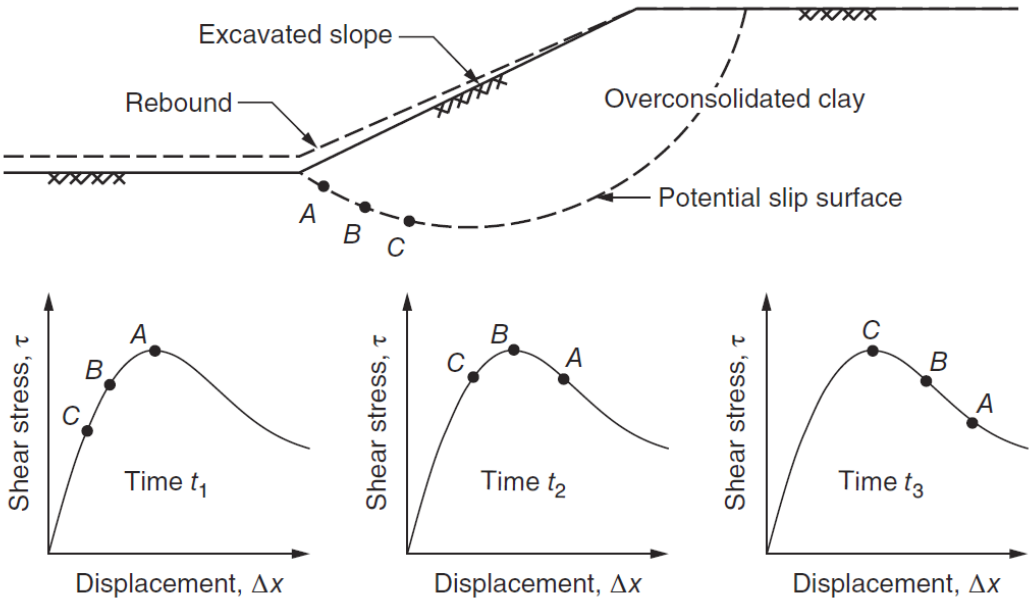

Figure 2.6. Progressive Failure of an Over-Consolidated Clay Slope (Duncan et al., 2014)

2.2.2. Dilatancy Effects on Failure of Retaining Walls

Another important aspect of retaining wall failure is related to dilatancy angle which is explained briefly. Studies have shown that real soil behavior does not match with associated flow assumption (Graham, Noonan, & Lew, 1983; Kirkgard & Lade, 1993) but mathematical modelling of associated flow is easier than non-associated flow (Krabbenhoft, Karim, Lyamin, & Sloan, 2012) due to asymmetry of constitutive and global stiffness matrices in non-associated case. (Potts & Zdravkovic, 2001)

Associated flow rule indicates plastic deformation at constant volume. Chowdhury (2009) states that associated flow rule only holds true for undrained soft clay behavior where $\phi=\psi=0$. Since volume of cohesive soils during undrained loading does not change due to rigidity of water particles, associated flow rule can reflect this behavior.

Many studies have been performed in Cambridge by Roscoe and his team on the rupture surface or failure surface orientation on sandy soils. Roscoe (1970) in his Rankine Lecture summarized their findings. Traditional method developed by

Coulomb (1773) assumes rupture surface coincide with stress characteristics where maximum stress plane lies on 45+ϕ'/2 direction. However, model tests on sandy soils in Cambridge shows that rupture surface coincide with velocity characteristics which is the direction of zero extension line. (Bolton & Powrie, 1988; Bransby, 1968; Bransby & Milligan, 1975; Roscoe, 1970) Zero extension line lies on the direction of 45+ϕ'/2 and identified by zero normal strain. Therefore, it can be concluded that soils with associated flow rule where ϕ=ψ obeys Coulomb's yield criteria since 45+ ϕ'/2 = 45+ψ'/2. However, for most type of soils, observed non-associated flow rule results in different failure direction than Coulomb's.

Bransby's (1968) model tests show the radiograph of rupture surface and direction of zero extension line.

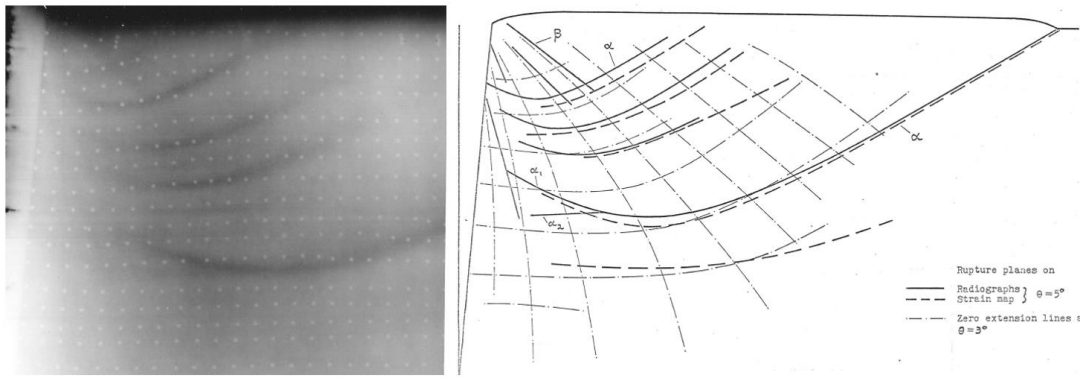

Figure 2.7.: Rupture Surfaces Observed in Model Test and Direction of Zero Extension Line (Bransby, 1968)

Chen & Liu, in their book "Limit Analysis in Soil Mechanics" (2012) states that Coulomb and other limit equilibrium solutions are based on stress characteristics. Therefore, critical failure surface in these analyses are not "representative of the actual failure surfaces." Coulomb and other limit equilibrium solutions' failure surfaces are based on stress characteristics; however, actual failure surface occurs through the velocity characteristics. These two states are equal only for associated cases and this

is the main and most misleading assumption of limit equilibrium solutions. Also, they emphasize on the procedure for back-analysis. For non-associated materials, back-analyses result will be based on the Davis (1968) parameters rather than Mohr-Coulomb parameters.

Similar conclusion has been drawn by Potts & Zdravkovic (2001) by performing associated and non-associated finite element analyses along with limit equilibrium solution on a 10m slope. Results confirm that limit equilibrium solutions are based on perfectly plastic material with associated behavior.

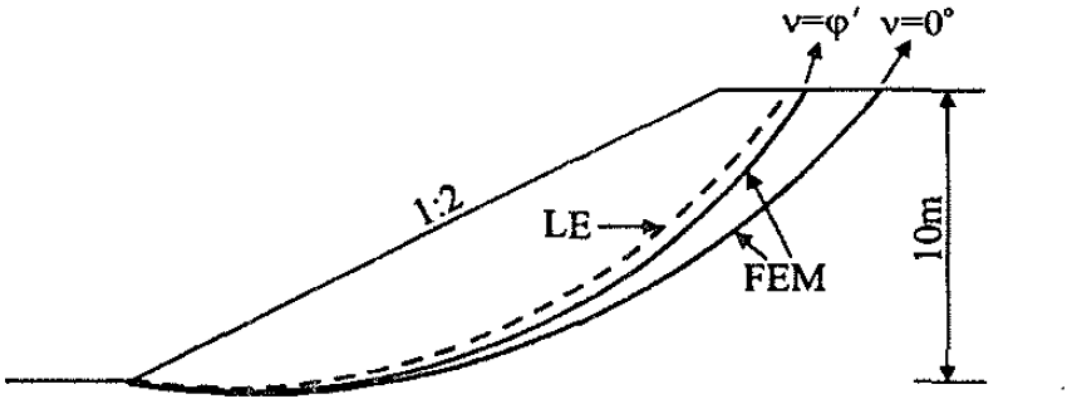

Figure 2.8.: Comparison of Different FEM Results with Different Dilation Angles and Limit Equilibrium Solution (Potts & Zdravkovic, 2001)

Potts & Zdravkovic (2001) gives the equation of acting shear stress on the rupture surface for non-associated materials:

$$\tau_f = \frac{c' \cdot \cos\phi' \cdot \cos\psi + \sigma_n' \cdot \sin\phi' \cdot \cos\psi}{1 - \sin\phi' \cdot \cos\psi} \qquad (10)$$

This equation is equal to Coulomb failure criteria for cases where ϕ=ψ. Based on this formulation, Davis (1968) developed an approach to model non-associated materials using theories based on associated flow rule. Since non-associated materials yield

lower factor of safeties, a reduction factor is defined for these materials. (Chen & Liu, 2012)

Tschuchnigg et. al. (2015), using Davis (1968) approach, developed three different procedure for strength reduction. In first approach, authors assumed Davis reduction factor remains constant throughout strength reduction. In second approach, since strength parameters are changed in every step of strength reduction procedure, reduction factor is re-calculated based on the updated parameters. Dilation angle is also reduced using the same rule. In third approach, dilation angle is kept constant while c and ϕ is reduced and reduction factor is re-calculated. Based on the analyses results, they concluded that first approach yields conservative results while second and third approaches are more realistic to represent non-associated materials using associated modelling techniques.

An important difference between associated and non-associated flow is solution uniqueness. For associated flow, solution is unique whereas for non-associated flow, solution to governing equations is not unique. (Tschuchnigg et al., 2015) Krabbenhoft et. al. (2012) discuss non-uniqueness behavior that results in oscillation in load displacement curve and based on the experimental research of Gajo et. al. (2004), they conclude that non-uniqueness of solution for non-associated materials is “real physics rather than mathematical pathology.” Gajo et. al. (2004) explains the oscillation behavior using the shear band concept, where with increasing load, new shear bands are formed that unload some of the stress on the soil. Oscillation behavior is shown in *Figure 2.9* by aforementioned three studies.

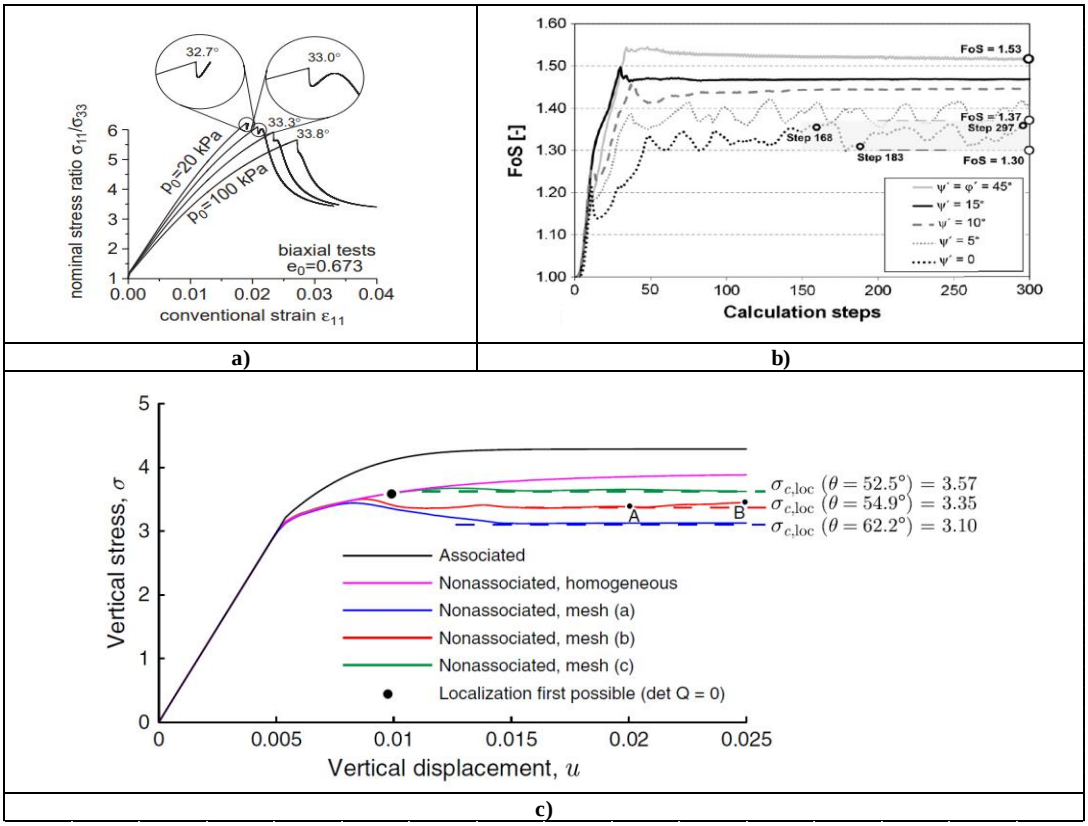

Figure 2.9. Oscillation Behavior in a) Gajo et. al. (2004) b) Tschuchnigg et. al. (2015) c) Krabbenhoft et. al. (2012)

2.2.3. Anchored Retaining Walls

Due to increasing depth of excavations, to limit deformations and increase factor of safety against overall stability failure, using lateral supports are very common in practice.

There are many methods to laterally support a retaining wall. Some of them are mentioned below:

- **Braced Excavations:** Excavation sides are connected using steel or reinforced concrete struts. Therefore, lateral forces from one side of the wall are used to support other side. Although rigidity of braces does not depend on the soil strength, passive or structural failures should be checked.

- **Raker Support:** If superstructure planning allows to partial construction of the building, central zone of the structure is built up to a point using simple excavation with berms. Then, rakers are connected to walls from building and berms are removed.
- **Top-Down Construction:** Basement columns and exterior walls are built from ground surface using techniques such as diaphragm wall. After that, excavation begins, slabs are formed to act as lateral supports.
- **Anchored Retaining Wall:** Although it is not the simplest method, anchored retaining walls are very popular in most countries including Turkey. Especially, increasing size of building footprints require anchored retaining walls since other methods require limited area. Anchors are installed at every excavation stage, after curing and pre-tensioning period next level excavations proceed. A diagram of the anchored retaining wall is given below.

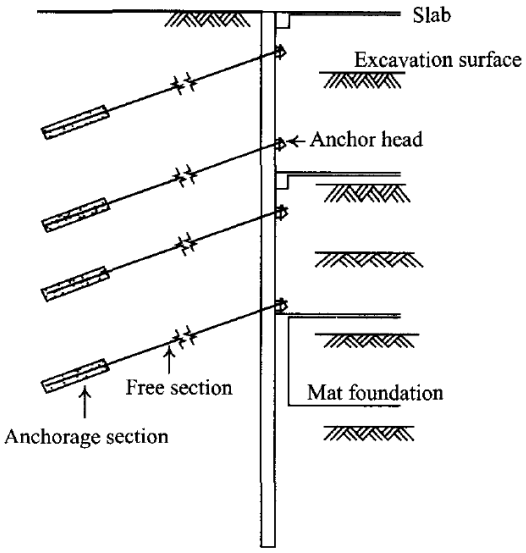

Figure 2.10. Anchored Retaining Wall Profile View (Ou, 2006)

Xanthakos (1991) states that the first ground anchors are utilized in Algeria for Cheurfas dam to stabilize the foundation using vertical ground anchors. Since then, ground anchors have been an integral part of geotechnical structures, both as tension bearing foundation elements and lateral supports for retaining walls.

Typical structure of a temporary ground anchor is presented below.

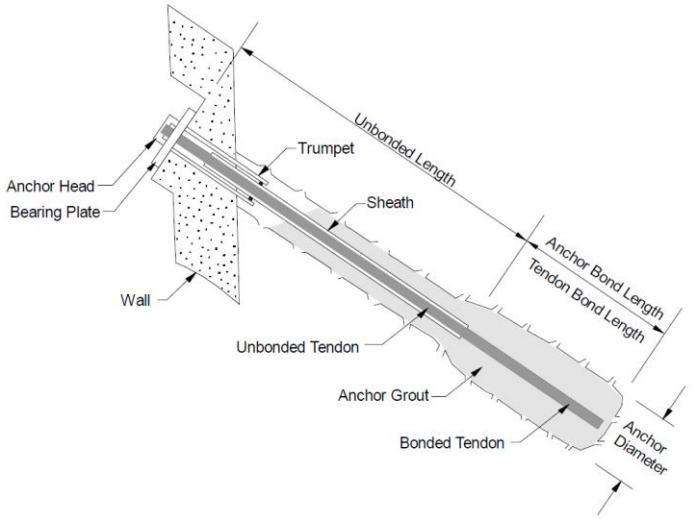

Figure 2.11. Typical Structure of Temporary Ground Anchor (Sabatini et al., 1999)

Failure modes of anchored retaining wall were detailed by FHWA-IF-99-015 (Sabatini et al., 1999). First three failure modes given in *Figure 2.12* corresponds to single anchor failure. Failure mode 'd' is related to structural capacity of the retaining wall and other modes are related to soil strength and stiffness.

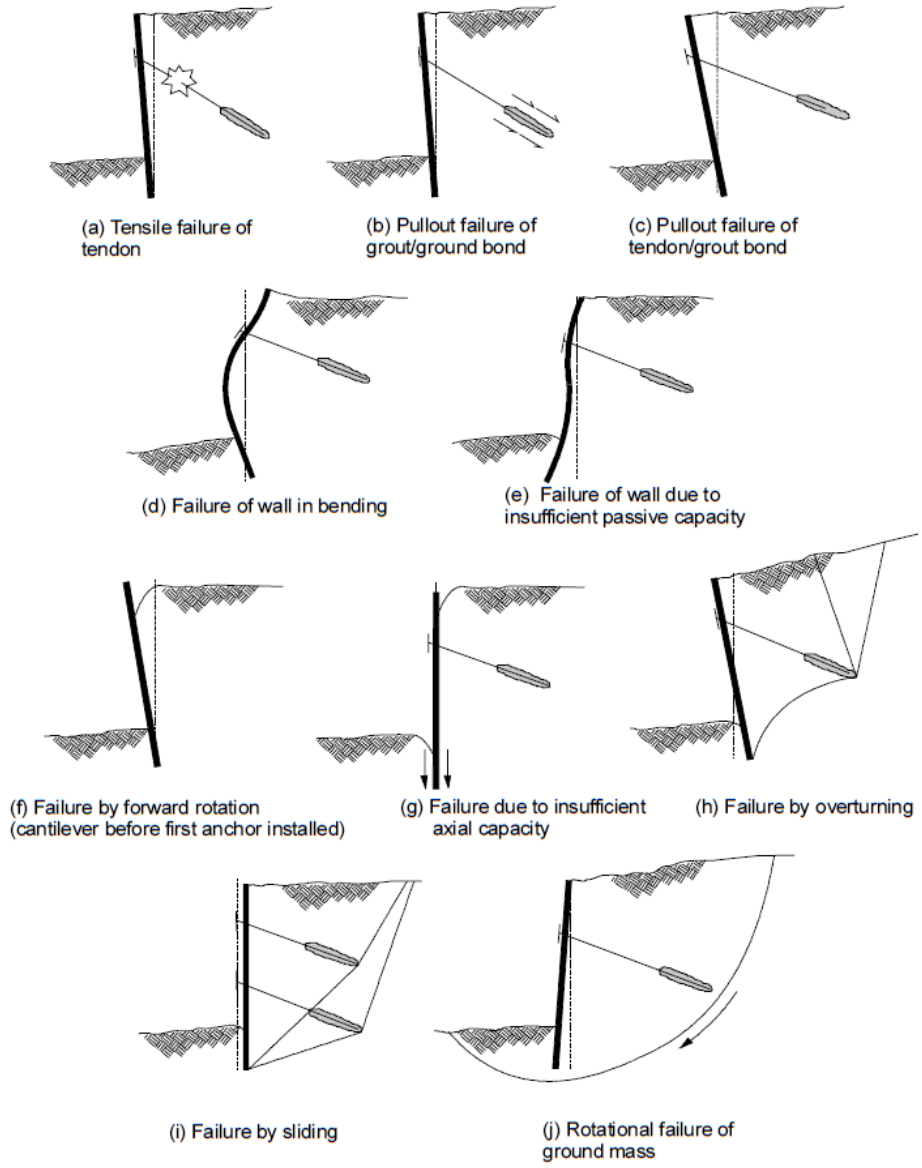

Figure 2.12. Failure Modes of Anchored Retaining Walls (Sabatini et al., 1999)

Construction scheme of a typical anchored retaining wall be summarized as below:

- Construction of retaining wall.
- First level excavation to -usually- 50cm-100cm below the first level anchor. (Cantilever stage)

- Drilling of anchor hole.
- Placement of anchor to the pre-drilled hole.
- Injection of cement-water mix to hole.
- Curing period.
- Testing of anchor as per the standards, typically to 150% to 200% of the design load.
- Pre-tensioning and locking the anchor to typically 110% to 125% of design load.
- Next level excavation to second anchor level.
- Same procedure continues till required depth of excavation.

Most important design parameters of anchors are length and angle from horizontal. Internationally accepted standards and books on this issue provide strict requirements and detailed guidelines. A detailed summary of these requirements and guidelines will be presented here:

- **FHWA-IF-99-015** (Sabatini et al., 1999)

FHWA Geotechnical Engineering Circular No:4 – Ground Anchors and Anchored Systems defines the area between failure surface and wall as "no load zone." Unbonded length should reach beyond "critical potential failure surface" by at least 0.2H or 1.5m where H is the depth of wall.

To determine failure surface, FHWA recommends $45+\phi'/2$ from the corner of excavation for cohesionless soil. For detailed analyses with ground anchors, sliding wedge force equilibrium or computer-based limit equilibrium solutions are recommended.

In case of failure surface passing through anchor bond length, FHWA recommends the procedure most Limit Equilibrium Codes implement, which is reducing the anchor force proportional to bonded length inside failure zone.

- **BS-8081** (British Standards Institution, 2015)

BS 8081:2015 – Code of Practice for Ground Anchors requires placement of anchor's bond length "beyond the critical failure surface" or "potential zone of ground rupture." Although 1989 version of the standard includes some recommendations on the determination of the failure surface, 2015 edition removed these recommendations.

- **Eurocode 7** (British Standards Institution, 2004)

Eurocode 7 – Part 1 – General Rules recommends placing anchor bond lengths "sufficiently distant" from the retained volume in order to "not adversely affect the stability".

- **Canadian Foundation Engineering Manual** (Canadian Geotechnical Society, 2006)

Canadian Foundation Engineering Manual requires not placing the anchors "within potentially deforming soil mass." Similar to FHWA, they recommend the same Rankine failure surface with at least 0.15H distance between bonded zone and failure surface.

- **Ou – Deep Excavation – Theory and Practice** (2006)

Ou clearly states that anchor bonded length should be at least 2m away from potential failure surface. He also summarizes most used potential failure surfaces. Previously stated additional anchor lengths are not included in the given figure, since these lengths are considered as safety precaution to theoretical failure surfaces.

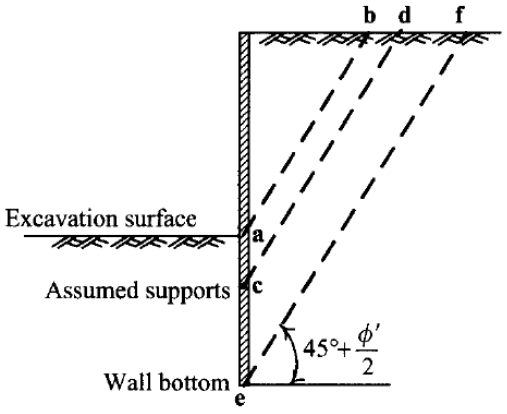

Figure 2.13. Recommended Failure Surfaces (Ou, 2006)

- **Clayton et. al. – Earth Pressure and Earth-Retaining Structures** (2014)

Clayton et. al. states that free length should be "adequate" to transmit the forces "far enough back from the wall." They also introduce Kranz method (Kranz, 1953). This method considers a planar failure surface within the bond length of anchor. Originally, method is developed for single dead-man anchored structures and initial assumptions exclude passive resistance of the wall and basal heave forces. Broms (1968) improved the method to include passive forces. (Juran & Elias, 1991)

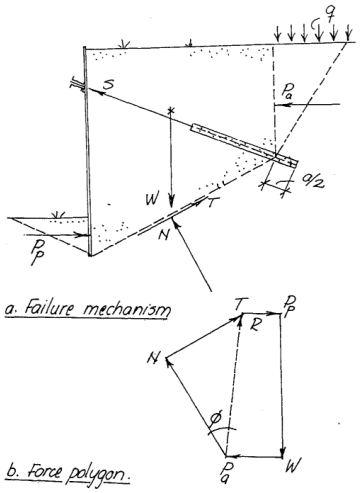

Figure 2.14. Kranz (1953) Method as Adapted by Broms (1988)

Similar statements that suggest placing the anchor bond length outside the failure zone can be found in the literature. (Anderson et al., 1983; Briaud & Lim, 1999)

Although there are some minor differences in the recommendations, common points may be listed as:

- All sources require anchor bonded length is placed outside of failure surface.
- All sources recommend Coulomb, log spiral or limit equilibrium surfaces. No final agreement on the determination of failure surface. (Ou, 2006)
- None of the sources differentiaes between stress and velocity characteristics.

Design of a single anchor includes several points that should be considered:

- **Design of ground-grout interface**

Design of ground-grout interface of anchors mainly depends on the empirical data provided in the literature. Appendix B of BS 8081 (British Standards Institution, 2015) provides an extensive collection of empirical data on different soil and rock types. FHWA-IF-99-015 (Sabatini et al., 1999) includes PTI's recommendations (Post-Tensioning Institute, 2004) for ultimate bond strength of different soil types. Although there are theoretical methods that relate pile capacity calculations to anchor ground-grout interface capacity, empirical solutions have been proven to be more reasonable. Besides, for all anchored retaining structures, there should be on site tests (such as suitability, acceptance etc.) to predict site specific capacity.

If no additions are used in the grout, modulus of elasticity of the grout can be assumed as 20 GPa.

- **Design of anchor strands:**

Earlier (1989) version of BS 8081 recommends 186 kN and 232 kN characteristic strengths for 0.5" and 0.6" strands respectively for 7-wire strands. 2015 version of BS 8081, recommends Eurocode 2 (European Committee for Standardization, 2004) and

Eurocode 2 recommends EN 10138 (European Committee for Standardization, 2005). This standard recommends 186 kN and 259 kN for 0.5" and 0.6" strands respectively. FHWA (Sabatini et al., 1999) and PTI (2004) recommends ASTM A416 (2017). ASTM A416 recommends 165.3 kN and 234.6 kN minimum load at 1% extension for Grade 270 steel strand of 0.5" and 0.6" respectively. Different tendon types are available at the market, therefore, aside from standardized recommendations, different characteristic yield strengths may be encountered. In this study, BS 8081 (British Standards Institution, 2015) recommendations will be used.

Modulus of elasticity of tendon may be accepted as 195 GPa as per the recommendations by EN 10138. However, in practice, anchor strands should be tested and design values should be selected as per the test results.

Another important point in the anchor design is elasto-plastic behavior of anchors. FHWA (Sabatini et al., 1999) describes anchor behavior using the following figure. Two possible case of anchor behavior due to ground-grout interface are shown by Case A and Case B. While Case A represents perfectly plastic case, Case B represents strain softening behavior.

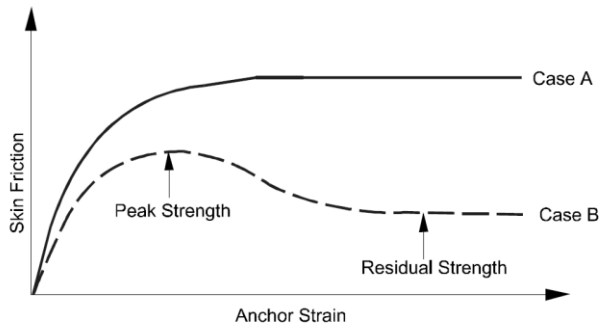

Figure 2.15. Elasto-Plastic Behavior of Anchors (Sabatini et al., 1999)

Do et. al. (2016) studied the difference between elastic and elasto-plastic strut models using 4 deep excavation failures (FS=1.00) and found that elasto-plastic strut models

fit better to field data while elastic strut models significantly over-estimates the factor of safety. Their results show that in cases of elasto-plastic structural elements, calculated factor of safeties are much closer to 1.00.

Table 2.2. Comparison of Elastic and Elasto-Plastic Strut Models by Do, Ou and Chen (2016)

Case history	Finite element method	
	Using elastoplastic structural elements	Using elastic structural elements
Taipei Rebar Broadway case	1.00	1.84937
Taipei Shi-Pai case	ΣM_{stage} = 0.6734 (at final excavation stage)	1.54807
Hangzhou Fengqing road case	ΣM_{stage} = 0.6652 (at final excavation stage)	3.07975
Nicoll highway case	1.13033	5.26420

2.2.4. Numerical Analysis Methods

Numerical techniques to solve geotechnical problems can be described in three parts as Cheng et. al. (2016) describes:

- Limit equilibrium methods
- Finite element limit analyses
- Displacement finite element methods

This section will cover these numerical methods in scope of the study. As Potts and Zdravkovic (2001) stated there are four conditions that should be satisfied in order to reach a complete numerical solution:

- Equilibrium
- Compatibility
- Material behavior
- Boundary Conditions

Therefore, these methods should also be evaluated based on the ability to meet these criteria for a complete theoretical solution as Potts & Zdravkovic (2001) presented.

Table 2.3. Comparison of Different Analysis Methods (Potts & Zdravkovic, 2001)

METHOD OF ANALYSIS		SOLUTION REQUIREMENTS				
		Equilibrium	Compatibility	Constitutive behaviour	Boundary conditions	
					Force	Disp
Closed form		S	S	Linear elastic	S	S
Limit equilibrium		S	NS	Rigid with a failure criterion	S	NS
Stress field		S	NS	Rigid with a failure criterion	S	NS
Limit analysis	**Lower bound**	S	NS	Ideal plasticity with associated flow rule	S	NS
	Upper bound	NS	S		NS	S
Beam-Spring approaches		S	S	Soil modelled by springs or elastic interaction factors	S	S
Full Numerical analysis		S	S	Any	S	S

S - Satisfied; NS - Not Satisfied

2.2.5. Limit Equilibrium Methods

Limit equilibrium methods (LEM) consider a pre-defined failure surface and calculates factor of safety by comparing shear strength along the failure surface with the calculated equilibrium shear stress. LEM considers equilibrium, however, calculations are performed only for failing mass. While force equilibrium is satisfied at the boundaries, no displacement-based analyses are included.

Some of the disadvantages of limit equilibrium methods can be listed as follows:

- Requirement to pre-define a failure surface.
- Assumption of mobilization of shear strength for all points on the failure surface.
- Lack of satisfaction of all equilibrium conditions for some methods.

- Equilibrium is not satisfied at every point but rather only on the slip surface. (Sloan, 2013)

Force equilibrium conditions to be satisfied in a limit equilibrium method are: (Duncan et al., 2014)

- Equilibrium of vertical forces
- Equilibrium of horizontal forces
- Equilibrium of moment about any point.

Nevertheless, limit equilibrium codes such as Rocscience Slide, GeoSlope Slope/W or UTexas4 are all found to be quite useful and accurate to calculate factor of safeties of slopes based on most common limit equilibrium methods. (Duncan et al., 2014)

2.2.6. Finite Element Limit Analysis

Finite element limit analysis (FELA) methods assume that soil is perfectly plastic with associated flow rule. FELA is solely based on materials with associated flow rule due to required normality of plastic strain vector to yield surface which is also called normality condition. (Chen, 1975)

Based on the given assumptions, unique failure surfaces can be determined based on either kinematically or statically admissible field assumption. However, it is theoretically proven that while kinematically admissible solutions that equate external work to internal energy dissipation approach to theoretical solution from above, statically admissible solutions that ensure no points in the domain has yielded approach to theoretical solutions from below. (Chen & Liu, 2012)

These solutions are named as upper bound and lower bound solutions in limit analyses literature. If two solutions are calculated, theoretical solution is “bracketed” from two sides. If two solutions are equal, exact solution is found. However, it is a rare case. In most cases, solution can be bracketed, and size of the bracket can be decreased by increased mesh properties.

Also, limit analysis methods do not consider displacements and construction sequence. (Potts & Zdravkovic, 2001) While FELA is only limited to associated materials, using Davis (1968) methods reasonable estimates for non-associated materials can be obtained. (Sloan, 2013; Tschuchnigg et al., 2015)

OPTUM G2 and G3 provides 2D and 3D solutions for finite element limit analysis along with displacement based finite element methods. (Krabbenhoft, 2018b)

2.2.7. Displacement Finite Element Methods

Displacement finite element method or as commonly known, finite element method is a solution technique that discretizes the solution domain into finite number of elements and solve the governing equations for the mesh points, which are also called nodes.

Potts and Zdravkovic (2001) define the steps of finite element technique as below:

- Element discretization: Dividing the domain into meshes. Elements used for meshes may change for each software. Plaxis 2D uses 6-node triangle and 15-node triangle. In this study, 15-node triangle is used due to better approximation using more nodes and stress points.

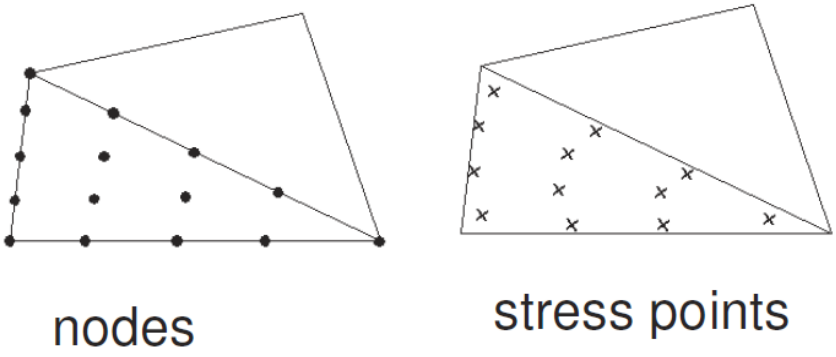

Figure 2.16. 15-node Element Nodes and Stress Points (Plaxis BV, 2017b)

- Primary variable approximation: Definition of variable may be selected as displacement or stress. For geotechnical engineering applications, it is

common to adopt displacement based procedure. (Potts & Zdravkovic, 2001)

- Element equations: Based on the Hooke principle (stiffness multiplied with displacement is equal to stresses), element equation for each node is created.
- Global equations: Using the same principles with element equations, global equations for solution domain are created.
- Boundary conditions: Determine the boundary conditions. For a plain strain, horizontal case; it is common to restrict the movement of side boundaries in horizontal direction. Bottom of the model is usually restricted in both direction.
- Solve the global equation: Displacements are obtained using the global equations. Using the obtained displacements, secondary values such as stress and strain can be calculated.

Strength reduction technique or safety analysis is used in most finite element software packages to reach a failure state using reduced parameters with a simple mathematical scheme. Strength parameters ϕ and c are decreased simultaneously to reach failure state. Ratio of initial parameters to reduced parameters is M_{sf} or factor of safety, FS. During safety analysis, dilatancy angle should be treated carefully to avoid excessive volume increase during failure. Plaxis reduces the ϕ only until $\phi=\psi$, after that point ϕ and ψ are reduced simultaneously. (Plaxis BV, 2017b) Also, during strength reduction, advanced soil models like HS or HSSmall are reduced to Mohr-Coulomb due to simplified assumptions. Mathematical expression of safety analysis is given below:

$$FS = \frac{\tan \phi_{input}}{\tan \phi_{reduced}} = \frac{c_{input}}{c_{reduced}} \tag{11}$$

CHAPTER 3

NUMERICAL ANALYSES

This thesis investigates the performance of short anchors after assuring that required factor of safety is provided with long anchors. Therefore, effect of long anchors on overall stability failure is not underestimated. However, common assumption is that only long anchors increase factor of safety and decrease deformations, and short anchors should not be used in any cases. This chapter questions this rule of thumb and discuss performance of short anchors after providing required factor of safety with long anchors.

Details of numerical analyses and their results are presented in this chapter. Due to significant differences on the results of finite element analyses and common misperceptions, first part compares different anchor modelling techniques. In the second part, performance of short anchors is compared with long anchors in various scenarios. In the third part, effect of dilatancy on the deformation and failure behavior of retaining wall is discussed.

Numerical analyses are carried out using Plaxis 2D 2017 Finite Element Package, unless otherwise stated. Since wedge analyses are mostly plane strain, 2D analyses are found to be satisfying for modeling purposes. Validations of 2D models are also performed for some scenarios using 3D FEM solutions. Hypothetical hardening soil parameters similar to those of normally consolidated Ankara Clay is chosen in the base model of this study, which are given in Table 3.1. Soil properties are assumed to be constant with depth. Any deviation from the base model is stated in the text.

Table 3.1. Base Soil Parameters

Unit Weight (kN/m^3)	$E_{50}=E_{oed}$ (kPa)	E_{ur} (kPa)	c' (kPa)	ϕ' (°)	ψ (°)	p_{ref} (kPa)	R_f	υ_{ur}	m	R_{inter}
19	50,000	150,000	8	25	0	100	0.9	0.2	1.0	0.85

Diaphragm wall is modeled using plate elements with special interface members in both sides and end-bearing correction at the tip to avoid unrealistic displacements. End-bearing correction is embedded in Plaxis to avoid punching of zero-thickness plate element in the soil by using equivalent diameter calculated using plate properties.

Elastic diaphragm wall model is used assuming rigid wall behavior. Effect of diaphragm wall modeling on the performance of short anchors is assumed negligible. This effect will be investigated in the next section.

80cm thick diaphragm wall (EA=24x106 kN/m and EI=1.28x106 kNm^2/m) is used throughout the analyses. For 30m excavation, diaphragm wall length is chosen as 45m to avoid passive failures and construction-stage failures. Also, deep embedment eases the distinction between short and long anchors.

In 2D analyses, anchors are modelled using node-to-node anchors for free length and geogrids for bond length. Following properties are used for anchors. Elastic properties of free lengths given as for per anchor and bond lengths (geogrids) are for per meter. Therefore, EA/m of bond length is divided to relevant horizontal spacing of anchors to obtain the stiffness parameters.

Table 3.2. Anchor Properties Adapted in the FE Analyses

Parameter	**Inputs**
Strand Type	3x0.6" seven-wire steel strand
Angle of Anchor with Horizontal	15°
Bond Length	8 m
E_{strand}	195 GPa
Maximum Anchor Capacity	777 kN
EA_{free} (EA of anchor free length)	81,315 kN/anchor
Pretension Load	350 kN
E_{grout}	20 GPa
EA_{bond} (per meter)	277,858 kN/m

For the safety analyses, phi-c reduction embedded in Plaxis is used and M_{sf} is taken as the safety factor. Step size in the safety analysis is increased to 250 from default value of 100 to observe the stabilization of safety factor curve. However, as described before, oscillation of load-displacement curve is common in non-associated materials. (Gajo et al., 2004; Krabbenhoft et al., 2012; Tschuchnigg et al., 2015) Therefore, reported safety factors are average of the last 50 steps.

Sides of the models are laterally fixed while bottoms of all models are fully fixed. Finite element method uses meshes to discretize the model space. 3022 soil elements and 24790 nodes are used to discretize the model space for 7L7S model with average element size 3.221m. Effect of different mesh densities are investigated using simple 7L model. Increasing the number of soil elements by a factor of approximately 2 has negligible effects (1% for lateral deformations and 0.2% for safety factor) on the results. Adapted mesh and boundary conditions are shown in the figure below for 7L7S model.

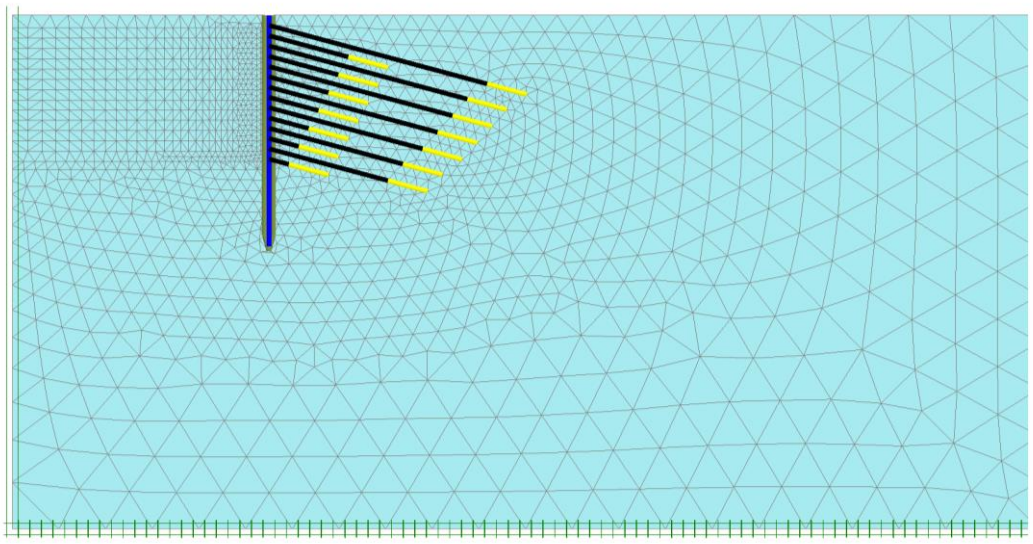

Figure 3.1. Boundary Conditions and Mesh View for 7L7S Model

3.1. Effect of Anchor Modeling on Retaining Wall Behavior

Anchors are composed of two parts: free length and bond length. In practice, free length should be encased in a PVC tube to avoid friction, while bond length is grouted fully to provide full interaction between soil and strands. To reflect these in finite element analyses, node-to-node anchor model is used in Plaxis to model free length while geogrid or -recently developed- embedded beams are used to model bond length. In this study, node-to-node anchor and geogrid models will be adopted as these are the most common.

Plaxis and most of other finite element packages offer three different anchor strand modelling: Elastic, elasto-plastic and elasto-plastic with residual strength. These models are compared based on their inputs and behavior.

Table 3.3. Comparison of Different Node-to-Node Anchor Models

Model Type	Inputs	Behavior
Elastic	EA and spacing	Elastic behavior. Capacity is not capped. Force on anchor is increased with increasing deformation.
Elasto-plastic	EA, spacing, F_{max} (tension and compression)	Elasto-plastic behavior. Capacity is capped. After reaching cap force, force on anchor stays constant with increasing deformation.
Elasto-plastic with residual strength	EA, spacing, F_{max} (tension and compression), F_{res} (tension and compression)	Elasto-plastic behavior. Capacity is capped. After reaching cap force, force on anchor drops to the given residual value and stays constant with increasing deformation.

Geogrid model also includes different behavior types such as elastic, elasto-plastic, elasto-plastic with user defined force-strain relationship and visco-elastic (time dependent) behavior.

To illustrate the common choice of private sector, 11 retaining wall designs performed in Turkey have been investigated. The investigated projects include deep excavations supported with anchors (10 case) and soil nails (1 case). Each excavation is designed by a different design company specialized in geotechnical design and/or construction. Results show that only 1 of 11 adopted elasto-plastic behavior in their design. Elastic model is used in other 10 cases and after final plastic stage, anchor forces are checked against strand and ground-grout interface capacity. Therefore, it is important to distinguish the behavior of elastic and elasto-plastic anchor behavior.

4 different models are created to examine the effect of anchor behavior on failure surfaces. Details of the models are summarized in table below. No Cap (NC) models implement elastic anchor modeling whereas Capped (C) models implement elasto-plastic model for the anchor strands and bonds. To simplify the subject, models that will be used in the following sections are considered in this comparison. More details

will be presented in the following chapters since anchor lengths and other details are not related to anchor modeling comparisons. Free length of long anchors (L) extend to 0.2H beyond the Rankine active failure wedge while short anchors (S) are inside the failure wedge.

Table 3.4. Comparison of Different Node-to-Node Anchor Models

Model Type	**Long Anchors**	**Short Anchors**	**Anchor Model**
7L-NC	7 Long anchors starting from -2.0 with 4 m vertical, 2 m horizontal spacing.	-	Elastic (No Cap)
7L-C	7 Long anchors starting from -2.0 with 4 m vertical, 2 m horizontal spacing.	-	Elastoplastic, strands capped at 777 kN and bond is capped at 800 kN/m.
7L7S-NC	7 Long anchors starting from -2.0 with 4 m vertical, 2 m horizontal spacing.	7 Short anchors starting from -4.0 with 4 m vertical, 2m horizontal spacing.	Elastic (No Cap)
7L7S-C	7 Long anchors starting from -2.0 with 4 m vertical, 2 m horizontal spacing.	7 Short anchors starting from -4.0 with 4 m vertical, 2 m horizontal spacing.	Elastoplastic, strands capped at 777 kN and bond is capped at 800 kN/m.

Using the 4 base models, results of different anchor models are compared. Failure surfaces are determined using total deviatoric strains. This results in similar surfaces with incremental deviatoric strains. Comparison of 7L-C and 7L-NC models are given in Figure 3.2.

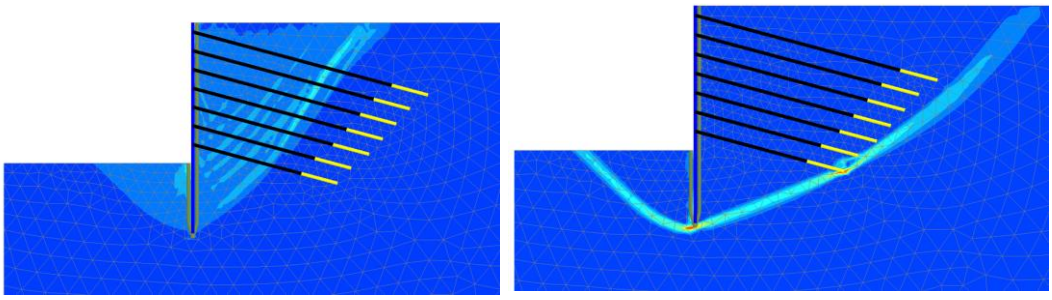

a) 7L - C **b) 7L - NC**

Figure 3.2. Failure Surfaces of a) 7L-C and b) 7L-NC Models

Similar comparison for 7L7S-C and 7L7S-NC models are also given in Figure 3.3.

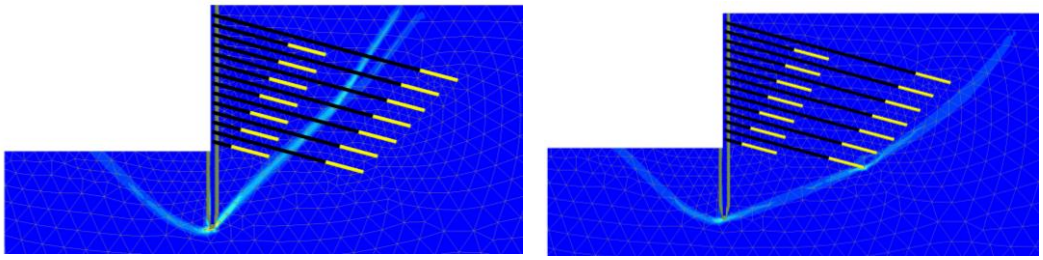

a) 7L7S - C **b) 7L7S - NC**

Figure 3.3. Failure Surfaces of a) 7L7S-C and b) 7L7S-NC Models

In addition to failure surface alignment, results are compared in Table 3.5. Safety factors (FS) of No Cap models are significantly higher than Capped models as expected.

Table 3.5. Comparison of Different Node-to-Node Anchor Models

Model Type	Capped Model	No Cap Model	Anchor Model
7L	1.291	1.700	31.6%
7L7S	1.373	1.551	12.9%

7L-C/NC and 7L7S-C/NC models' failure surfaces at the end of phi-c reduction stage are given in Figure 3.2. and Figure 3.3. Infinite loading of elastic anchors during safety phase shifts the failure surface to outside of anchored zone in No Cap models. However, anchors have only limited capacity, thus, if density of anchors is not high, failure plane passes between wall and bonded length by destroying the anchor strands.

Also, elasto-plastic anchor model allows developing shear bands between failure surface and wall which agrees with observations in model studies. (Bransby, 1968; Bransby & Milligan, 1975) However, infinite strength of elastic anchors does not allow any shear bands or minor failure surfaces inside the failure wedge.

In No Cap models, long anchors are loaded until soil at the tip of the bonded length fails before Rankine failure surface is activated. However, in capped model, limited anchor capacity allows mobilization of shear strength of soil along failure surfaces that vary between stress and velocity characteristics based on the degree of non-associativity.

Results clearly show that elasto-plastic support model should be used for modeling the failure of anchor-supported retaining structures. Otherwise, unrealistic excessive loads on the anchors may result in incorrect failure surfaces. However, it is crucial to obtain correct failure surface not only to obtain correct FS, but also to take necessary measures to increase factor of safety where it is lower than accepted limits.

As stated before, design practice in private sector mostly depends on elastic material behavior. In this case, designer checks the failure surface and safety factor. If safety factor is lower than accepted limits (such as 1.5), designer will revise the anchor or

wall configurations. In elastic case, designer will increase the length of the anchors to increase the safety factor. In fact, since NC (elastic) models are based on the wrong assumptions, i.e. failure surface shifts even more due to elastic anchor model and due to increased length of the failure surface, factor of safety increases. However, in reality, which is more similar to Capped models, failure surface passes through between bonded parts of long anchors and the wall. Therefore, increasing the anchor length does not increase factor of safety in Capped models and also in reality. However, designer who uses elastic model may, mistakenly, think that safety factor is increased. Instead, number of anchors or strength of anchor material should be increased to delay the yielding of anchors.

In addition, as reported before, safety factors of elastic models are significantly higher than elasto-plastic models. Therefore, elastic models over-estimate the safety factor and may result in terrible consequences such as overall stability failure.

Do et. al. (2016) reached similar results by comparing the elastic and elasto-plastic strut modeling for 4 deep excavation failures. They concluded that elastic strut systems used in back analyses of excavation failures overestimate the safety factors while elasto-plastic systems provide more accurate results. Analyses presented above agree with their results. Therefore, all other analyses in this study adopts elasto-plastic anchor models.

3.2. Performance of Short Anchors Inside the Failure Wedge

In all cases that consider deep excavations, long anchors should be used to avoid overall stability failure. However, after certain number of long anchors, factor of safety may increase above the required limit, but deformations may still be higher than tolerable limits.

In this section, by considering different scenarios, performance of short anchors will be compared with long anchors. It is a well-known fact that long anchors reach outside the failure surface to “tie” the failure wedge to soil behind the failure wedge to avoid overall stability failure. This study questions the rule that short anchors, under any circumstances, should not be used. To do that, 3 base models are created. 7L model which only includes 7 long anchors that reach behind the failure wedge is the base model. In addition to 7 long anchors, 7 short anchors are included, and this model is named as 7L7S. Lastly, 14L model is created with additional 7 long anchors to base 7L model.

View of anchor lengths for three models are given in Figure 3.4. Also, detailed anchor lengths and depths are given in Table 3.6.

To make sure that long anchors are outside the failure wedge, most conservative failure surface with rigid wall assumption which is described in previous chapters is adopted. To be on the safe side, for anchor length calculations only, ϕ is taken as 0. For short anchors, safety length (1.5m or H/5, whichever is highest) is omitted.

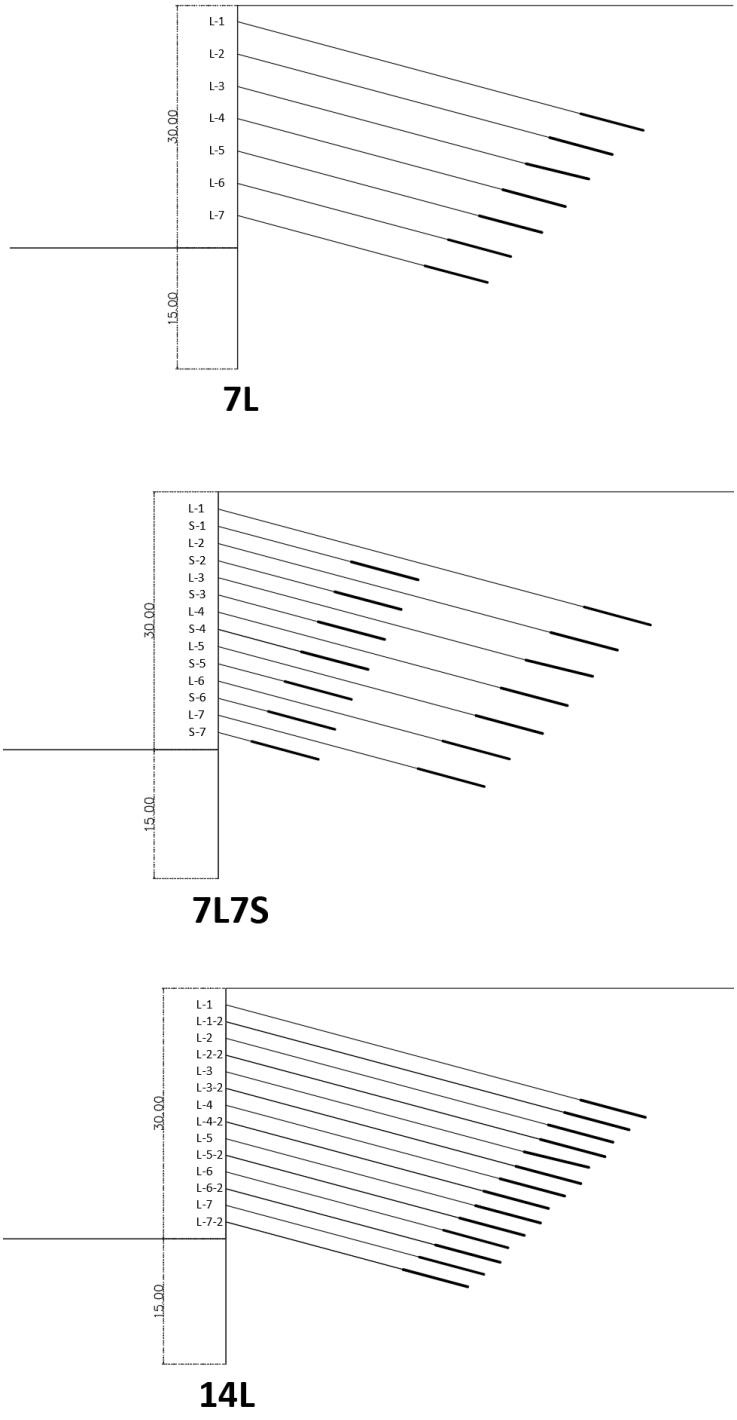

Figure 3.4. Model Views of 7L, 7L7S and 14L Models

Table 3.6. Anchor Lengths Used in Base Models

Model Name	Free Length	Bond Length	Total Length	Depth
7L Model	44	8	52	2
	40	8	48	6
	37	8	45	10
	34	8	42	14
	31	8	39	18
	27	8	35	22
	24	8	32	26
7L7S Model	44	8	52	2
	16	8	24	4
	40	8	48	6
	14	8	22	8
	37	8	45	10
	12	8	20	12
	34	8	42	14
	10	8	18	16
	31	8	39	18
	8	8	16	20
	27	8	35	22
	6	8	14	24
	24	8	32	26
	4	8	12	28
7L7S Model	44	8	52	2
	42	8	50	4
	40	8	48	6
	39	8	47	8
	37	8	45	10
	36	8	44	12
	34	8	42	14
	32	8	40	16
	31	8	39	18
	29	8	37	20
	27	8	35	22
	26	8	34	24
	24	8	32	26
	22	8	30	28

Different scenarios are considered for model comparisons. These scenarios include equal anchor quantity comparison, equal addition to 7L model and constant horizontal spacing comparison.

Equal anchor quantity comparison considers same anchor quantity for unit meter of diaphragm wall. To do that without changing the geometry of base models, different horizontal spacings are calculated for each model to reach equal anchor quantity per unit meter of wall.

Equal addition to 7L model compares performances of additional 7 short anchors to 7L model which is 7L7S and additional 7 long anchors to 7L model which is 14L. Again, not to alter with the geometry of base models, horizontal spacings are varied. 7L model with 2m horizontal spacing is kept constant and by changing the horizontal spacing of additional anchors, equal addition to 7L model condition is met.

Lastly, all models' horizontal anchor spacings are fixed at 2m. Comparisons are performed by considering total quantity vs. increase in factor of safety and decrease in lateral deformations.

Details of each model will be presented in the corresponding chapters.

3.2.1. Equal Anchor Quantity Comparison

In the first case, anchor quantities per unit meter of the wall are the same. This comparison is performed to develop a practical sense on the performance of the short anchors. Three different models imply that designer may select one of the followings:

- Wider vertical spacing and shorter horizontal spacing with long anchors as 7L model.
- Shorter vertical spacing and wider horizontal spacing with long anchors as 14L model.
- Shorter vertical spacing and medium horizontal spacing with combination of short and long anchors as 7L7S model.

Details of equal anchor quantity comparison are given below.

Table 3.7. Details of Equal Anchor Quantity Comparison

Model Name	Total Anchor Quantity (A)	Horizontal Spacing (B)	Anchor Length Per Meter (A/B)
7L-s2	293m (7L)	2m	146.5 m/m
7L7S-s2.86	293m (7L) + 126m (7S)	2.86m	146.5 m/m
14L-s3.93	293m (7L) + 282 (7L)	3.93m	146.5 m/m

Results of the equal anchor quantity models are also presented below.

Table 3.8. Results of Equal Anchor Quantity Comparison

Model Name	Max. Lateral Deformation (cm)	Factor of Safety
7L-s2	22.42	1.291
7L7S-s2.86	16.66	1.313
14L-s3.93	21.86	1.265

Moreover, vertical deformation profiles along a 50m line behind the retaining wall of each models are compared. As expected, 7L7S model's vertical deformation is lower than others.

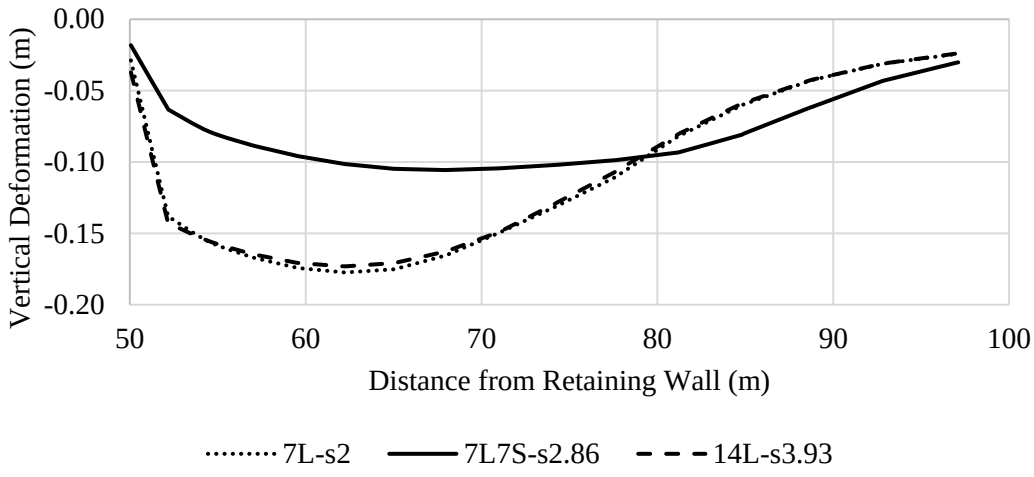

Figure 3.5. Comparison of Vertical Deformation Profiles

Bending moment comparison of 3 models are given in Figure XX. Although the differences are not high, 7L7S model yields the smallest bending moment.

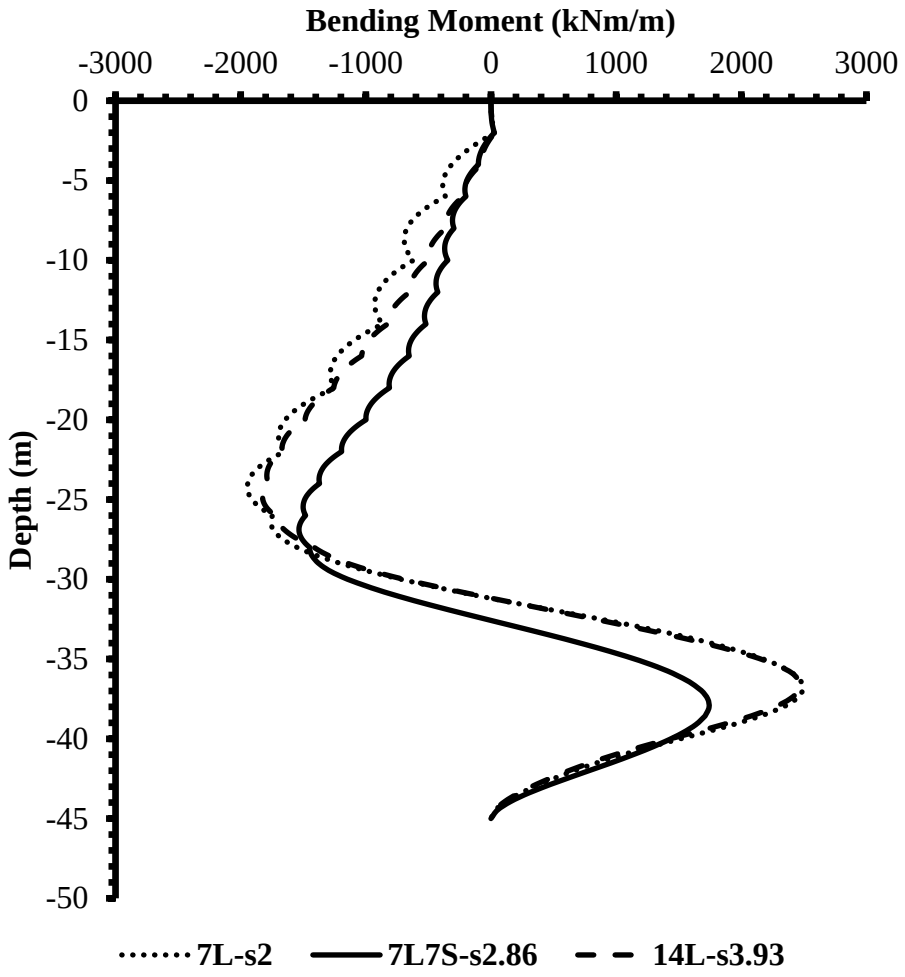

Figure 3.6. Bending Moment Comparison of Last Serviceability Stage

Results show that factor of safety of 7L7S model is slightly higher than 7L and 14L models. This is an important outcome considering many recommendations in the literature against short anchors. The reason of higher factor of safety of 7L7S model is redistribution of forces between anchors in the safety analysis. Since anchors are

modelled with elasto-plastic material properties, failure strongly depends on the maximum capacities of anchors and steps at which anchor loads reach these capacities. For 7L and 14L models, since anchors are widely spaced (8 m^2/anchor), loads on each anchor increases rapidly. However, for 7L7S model, short anchors also carry some of the active pressure of the wall, therefore, reducing the loads on the long anchors and delaying the step at which all anchors are loaded up to their capacity. Therefore, short anchors do not increase the factor of safety *per se*, but instead, by decreasing the loads on the long anchors, delay the failure of long anchors and eventually increase the factor of safety. Anchor loads at the final serviceability phase before the phi-c reduction are compared to prove these interpretations. *Figure 3.7* shows that anchor loads at 7L7S models are significantly lower than others due to high density of anchors. Another important outcome of this figure is that short anchors are loaded by a factor of 20% less than long anchors. This is also logical since long anchors tie the failure wedge to the back which results in higher demand. Therefore, based on this limited case, it can be assumed that short anchors to reduce displacements can be designed with lesser capacity than long anchors, if similar results are obtained through the detailed numerical analyses.

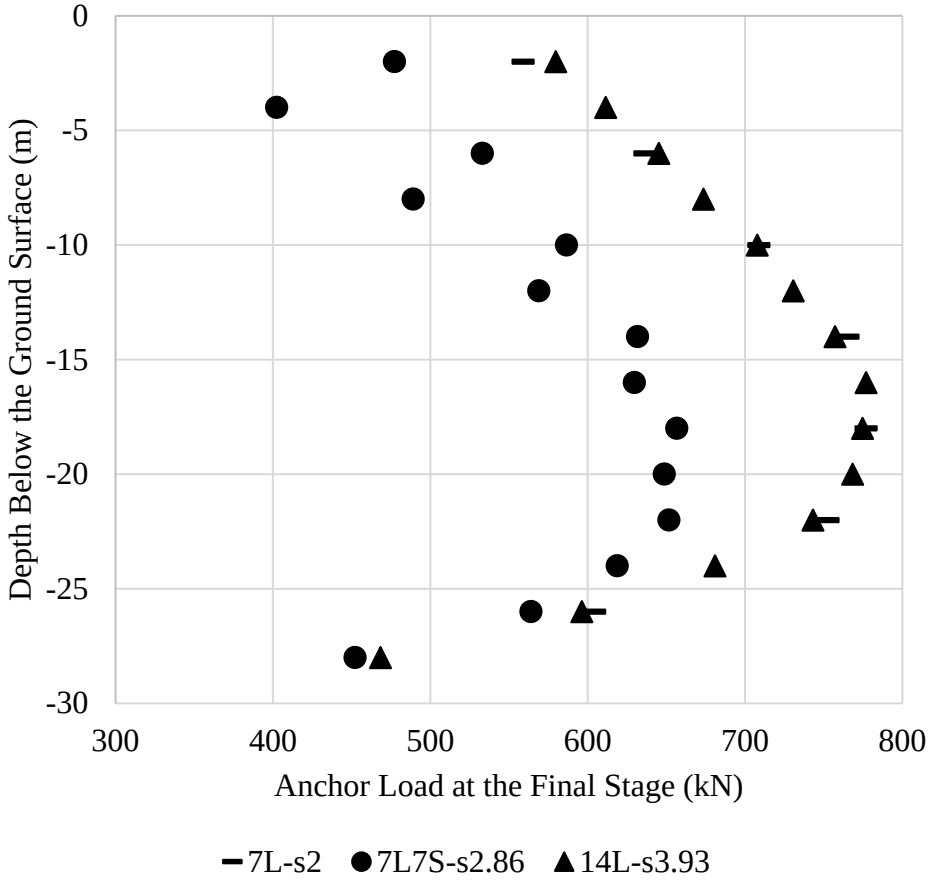

Figure 3.7. Anchor Loads at Last Serviceability Stages

Another reason for the increase in 7L7S model's factor of safety compared to that of the others can be found in the shear band theory. As the failure wedge is loaded up to failure, new shear bands form between the failure surface and the wall. (Bransby, 1968; Bransby & Milligan, 1975) Since bond lengths of short anchors are placed inside these zones, new shear bands are prevented. Long anchors do not affect these surfaces since anchor strands are modelled using node-to-node anchors that only transfer the load between two points which is a fair representation of the actual case. However, it should be noted that degree of improvement of minor shear bands decreases in 3D analyses since these minor bands are formed between individual short anchors. In 2D analyses, due to 2D nature of the problem, these bands are improved

with plain strain node to node anchors, however, 3D implementation is more realistic. Total deviatoric strains of 7L, 7L7S and 14L models are presented below below for last serviceability stage and phi-c reduction stage separately. Since a logical scale cannot be found for phi-c reduction stag, same-scale comparison is given for serviceability comparisons only. For phi-c reduction comparisons, only the alignment of failure surfaces should be regarded. Shear bands in 7L and 14L models can be observed between failure wedge and wall, while only a few shear bands formed in the same area for 7L7S models.

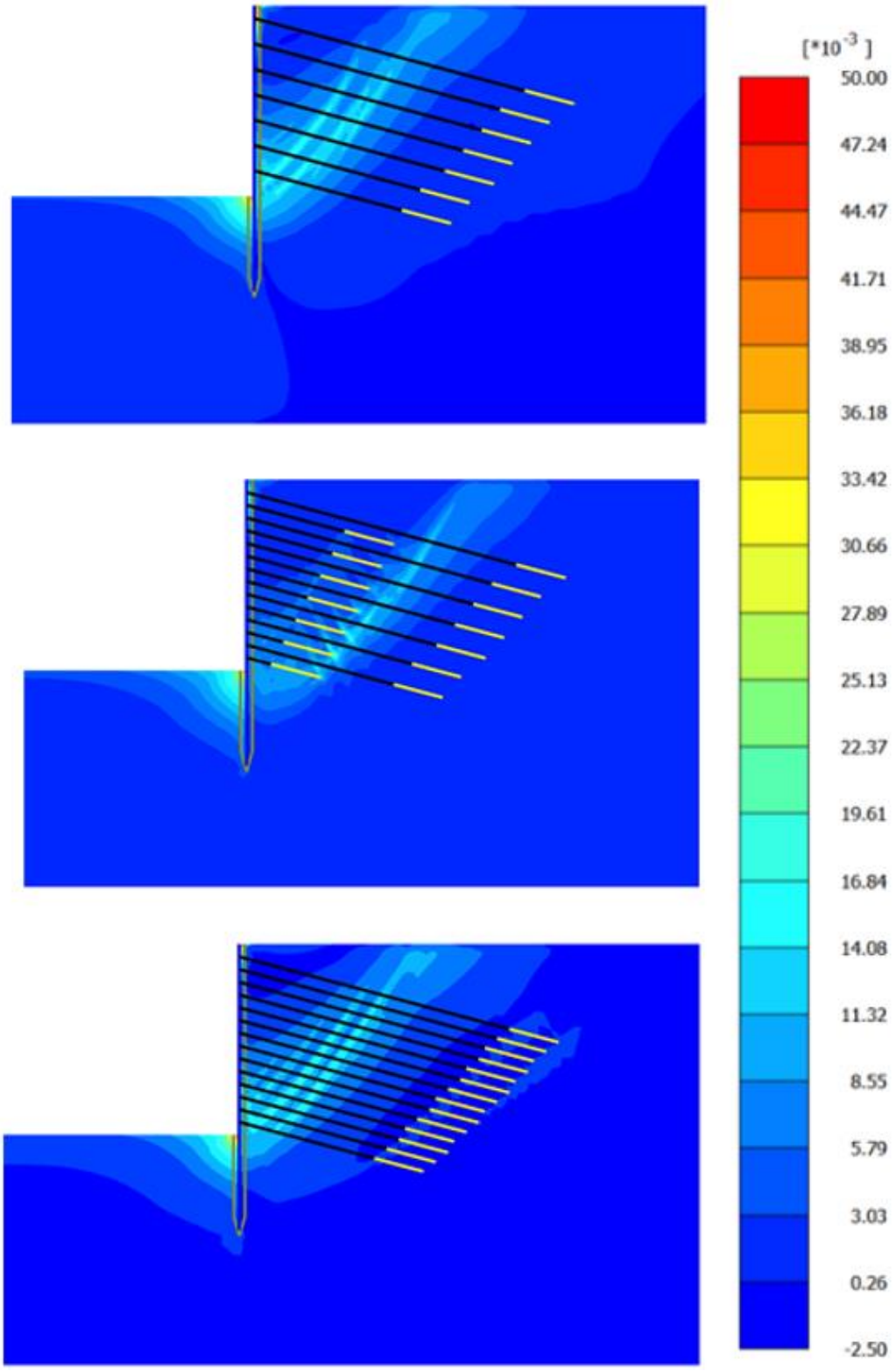

Figure 3.8. Total Deviatoric Strains of 7L, 7L7S and 14L Models at Last Serviceability Stage

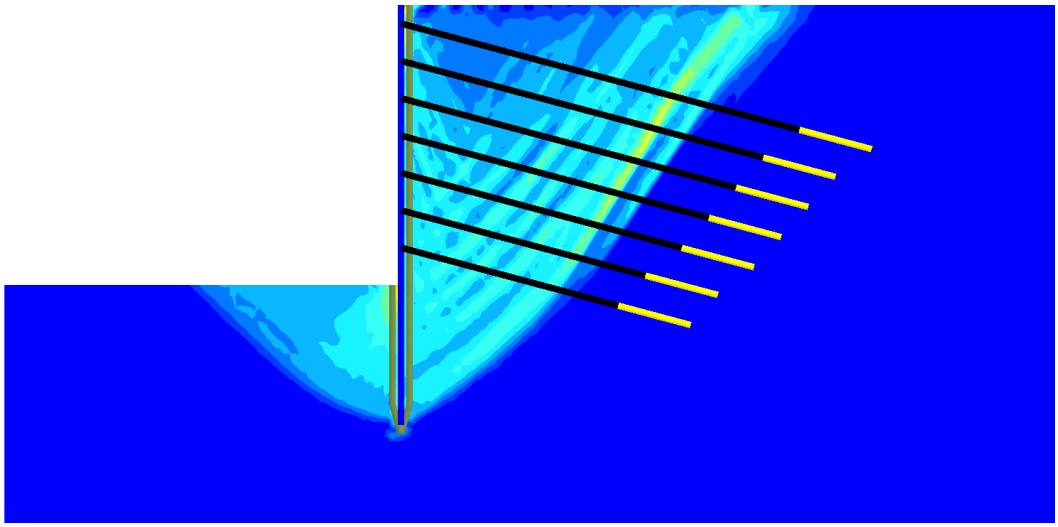

Figure 3.9. Total Deviatoric Strains of 7L-s2 Model at Phi-c Reduction Stage (Log scale)

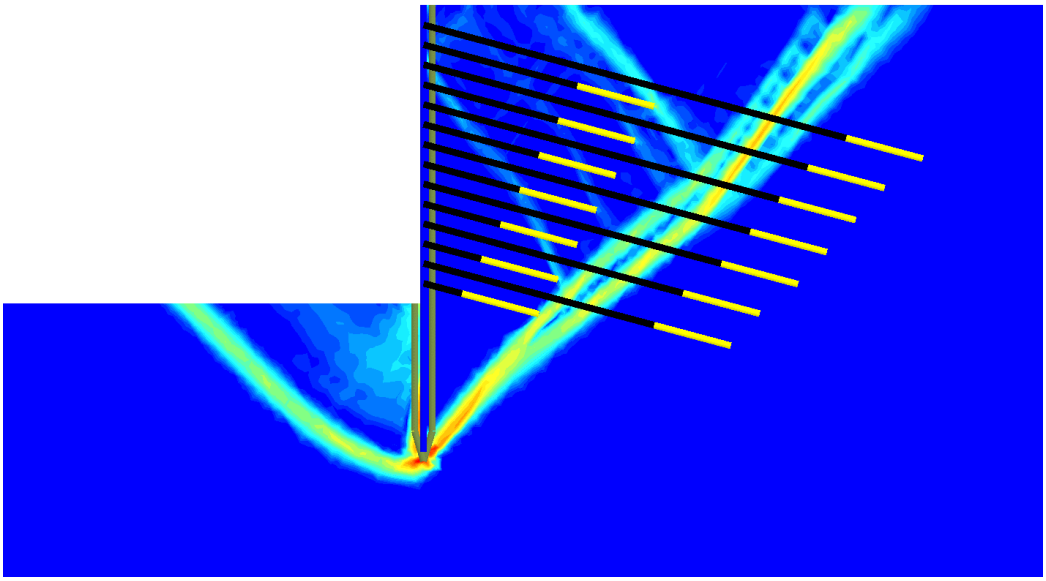

Figure 3.10. Total Deviatoric Strains of 7L7S-s2.86 Model at Phi-c Reduction Stage (Log scale)

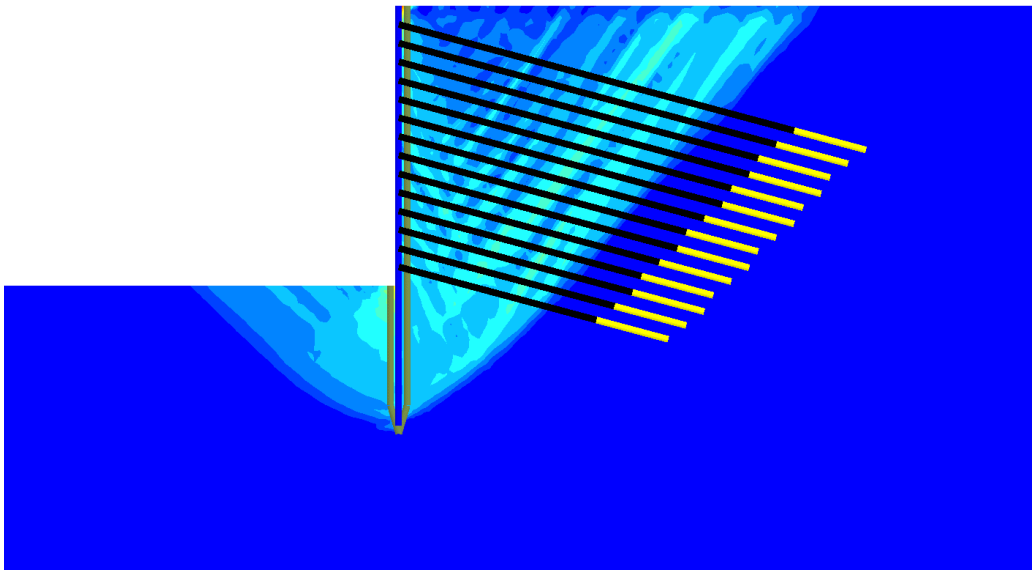

Figure 3.11. Total Deviatoric Strains of 14L-s3.93 Model at Phi-c Reduction Stage (Log scale)

Most important result of equal anchor quantity comparison is the significant difference between maximum lateral deformations for three cases. Results show that for three cases with equal quantity of anchors, 7L7S model's maximum lateral deformation is significantly lower (around 25%) than alternatives with only long anchors.

Equal anchor quantity comparisons have been also performed using Plaxis 3D 2016.2 (2017c) to check the results and validate the 2D procedure. Similar assumptions with 2D model have been adapted in 3D model, also. Model dimensions are selected to use 10 anchors in transverse direction with s/2 spacing left between last anchor and boundary. Model dimension in longitudinal direction is 150m.

Analyses yield similar results for 7L and 14L models, however, for 7L7S model, 3D factor of safety is higher than 2D. Outer failure surface behind the long anchors are activated, but failure surface in 2D analyses is still the governing failure surface. Results have been compared in Table 3.9.

Table 3.9. 2D vs. 3D Comparison of Equal Anchor Quantity Comparison Results

Model Name	Max. Lateral Deformation (cm)		FS	
	2D	3D	2D	3D
7L-s2	22.42cm	21.68cm	1.291	1.319
7L7S-s2.86	16.66cm	17.62cm	1.318	1.426
14L-s3.93	21.86cm	21.13cm	1.281	1.304

It is also noticed that required steps to reach stabilized factor of safety are significantly higher in 3D analyses compared to 2D analyses. Maximum step of 7L and 14L models is increased to 1000 and after 600th steps solution is stabilized. However, 7L7S model exhibits slow convergence, thus maximum step is increased to 1850 and solution is stabilized after only 1600th steps.

Failure surfaces of 3D models using incremental deviatoric strains have been shown in the figures below. Irregularity of shear bands in 7L7S model is due to bond lengths of short anchors which eventually increased the factor of safety.

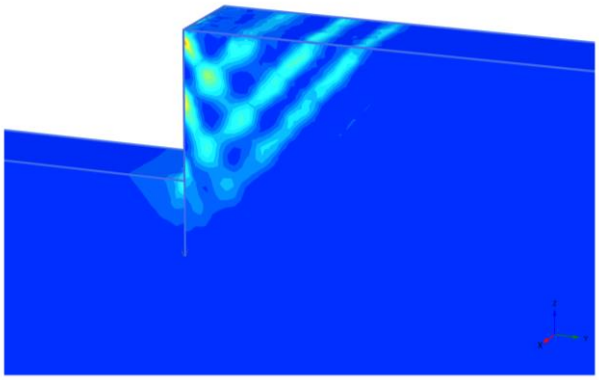

Figure 3.12. Incremental Deviatoric Strains of 7L-s2-3D Model

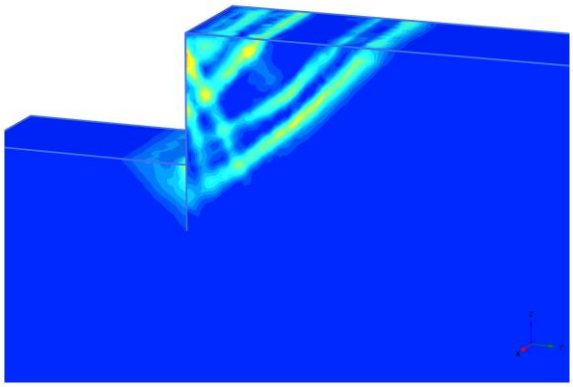

Figure 3.13. Incremental Deviatoric Strains of 7L7S-s2.86-3D Model

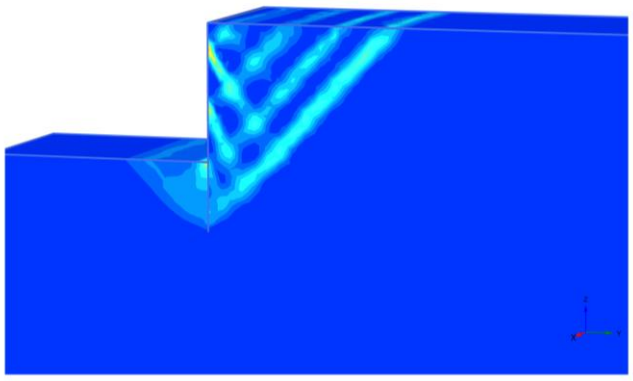

Figure 3.14. Incremental Deviatoric Strains of 14L-s3.93-3D Model

Lastly, effects of rigid wall assumption on the conclusions derived from equal anchor quantity comparison are investigated. Elasto-plastic plate is used to model flexible wall with moment capacity equals to 3000 kNm/m which indicates heavily reinforced diaphragm wall for 80cm thickness. This value is selected such that all moments during serviceability analyses are in elastic range so that effect of elasto-plastic wall model on the failure behavior can be assessed during ultimate limit state calculations.

Results are presented below. Due to flexibility of the retaining wall, a secondary failure surface develops through a hinge between excavation bottom and toe of the

wall as defined before. (*Figure 3.15*) Dominating failure surface can be developed either through the hinge or through the toe of the wall based on the moment capacity of the wall. Low moment capacity will induce hinge failures earlier which may reduce the demand on the soil strength. However, high moment capacity of retaining wall will increase the demand on the soil strength which may trigger the failure surfaces presented for rigid/elastic wall assumption.

Elasto-plastic wall calculations are not performed for SLS since as normal practice, designer will check the moment demand and design the reinforcement according to. Therefore, SLS results will be same for both elastic and elasto-plastic walls and anchors if demands during SLS are lower than capacity. The effect of elasto-plastic behavior is pronounced during ULS.

The main reason for assuming rigid wall behavior during main analyses is to aim of defining a clear distinction between short and long anchors. Single or double hinge failures (*Figure 3.15*-c) of retaining walls may result in intersection of some short anchors' bond lengths with failure surfaces which may cause wrong interpretations as shown in *Figure 3.15*-b. However, comparison of elastic and elasto-plastic wall safety factors show that same conclusion still applies to elasto-plastic wall case too.

Table 3.10. Results of Equal Anchor Quantity Comparison with Elastic and Elasto-Plastic Wall

Model Name	**FS Elastic Wall**	**FS Elasto-Plastic Wall**
7L-s2	1.291	1.125
7L7S-s2.86	1.313	1.142
14L-s3.93	1.265	1.265

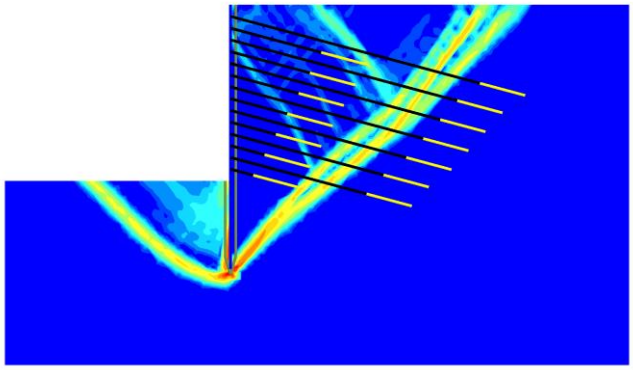

(a)

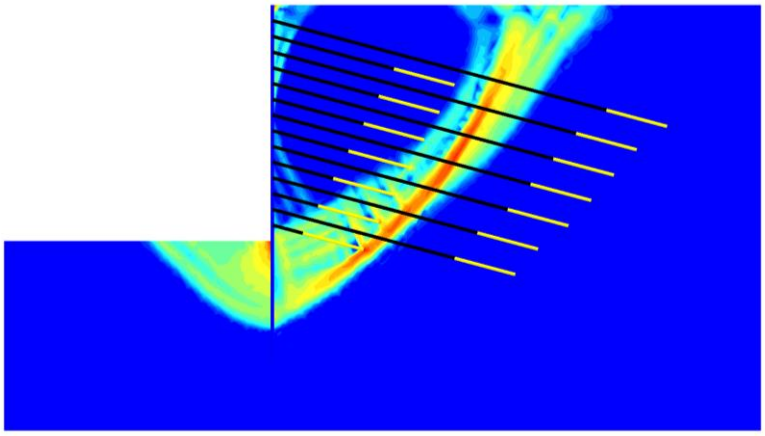

(b)

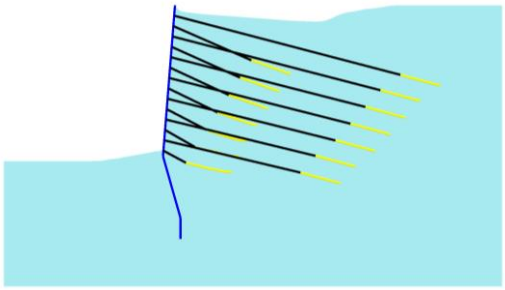

Figure 3.15. 7L7S-s2.86 Model Failure Surfaces, a) Elastic Wall b) Elasto-Plastic Wall c) Elasto-Plastic Wall Failure Behavior

3.2.2. Equal Addition to 7L Model

A different scenario with equal anchor addition to 7L model is considered. 7L model is kept same with 2m horizontal spacing while additional anchors included in 7L7S and 14L models compared to 7L model are kept at same quantity. For 7L7S model, horizontal spacing is kept constant for both short and long anchors at 2m. Therefore, additional anchor quantity to 7L model is 63 m/m. To keep the additional long anchor quantity for 14L model same with the 7L7S model, horizontal spacing of additional long anchors in 14L is changed to 4.48m. Therefore, both model increase the anchor quantity of 7L by 63 m/m. Details of the models are presented below.

Table 3.11. Details of Equal Addition to 7L Model

Model Name	**Total Anchor Quantity**	**Additional Anchor Quantity**
7L-s2	293m (7L) / 2m	-
7L7S-s2-2	293m (7L) / 2m + 126m (7S) / 2m	63 m/m
14L-s2-4.48	293m (7L) / 2m+ 282 (7L) / 4.48m	63 m/m

Results of equal addition to 7L model are presented below.

Table 3.12. Results of Equal Anchor Quantity Comparison

Model Name	**Max. Lateral Deformation (cm)**	**Percent Difference with 7L**	**Factor of Safety**	**Percent Difference with 7L**
7L-s2	22.42	-	1.291	-
7L7S-s2-2	11.68	-48%	1.373	6%
14L-s2-4.48	13.82	-38%	1.469	14%

Results show that, by keeping the additional anchor quantity same, short anchors decrease the maximum lateral deformation by 48% while long anchors decrease by 38%. Therefore, it can be concluded that if overall stability is ensured using long anchors -in this case 7 long anchors- short anchors are more effective -25% better-

than long anchors in terms of lateral deformation. As expected, effect of additional long anchors is more pronounced than short anchors for factor of safety, however, no negative effect is observed with short anchors on the overall stability behavior, instead 6% increase is observed.

This scenario is similar to real-life scenarios where designer is satisfied with Factor of Safety while lateral deformations are higher than limits. In this case, lateral deformations are around %0.74H while 7L7S and 14L models decrease the deformations around %0.4H which is acceptable for anchored retaining walls in most international standards including Turkey.

Bending moments with depth for each model are given in Figure XX and lateral deformations with depth for each model are given in Figure XX. Results show that 7L7S model performs better than 14L in terms of lateral deformations and approximately same in terms of bending moment with 14L model.

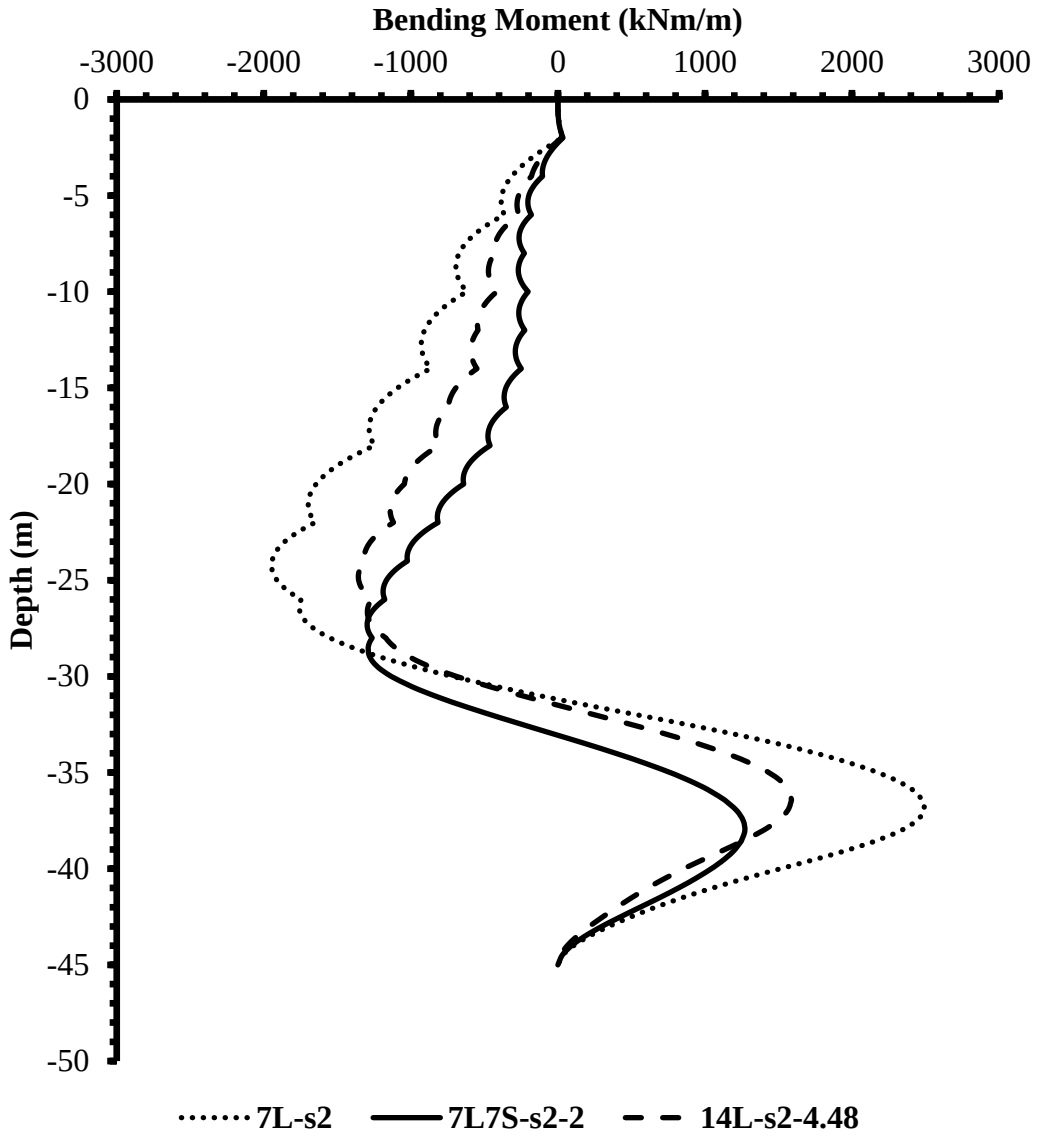

Figure 3.16. Comparison of Bending Moments for Equal Addition Models

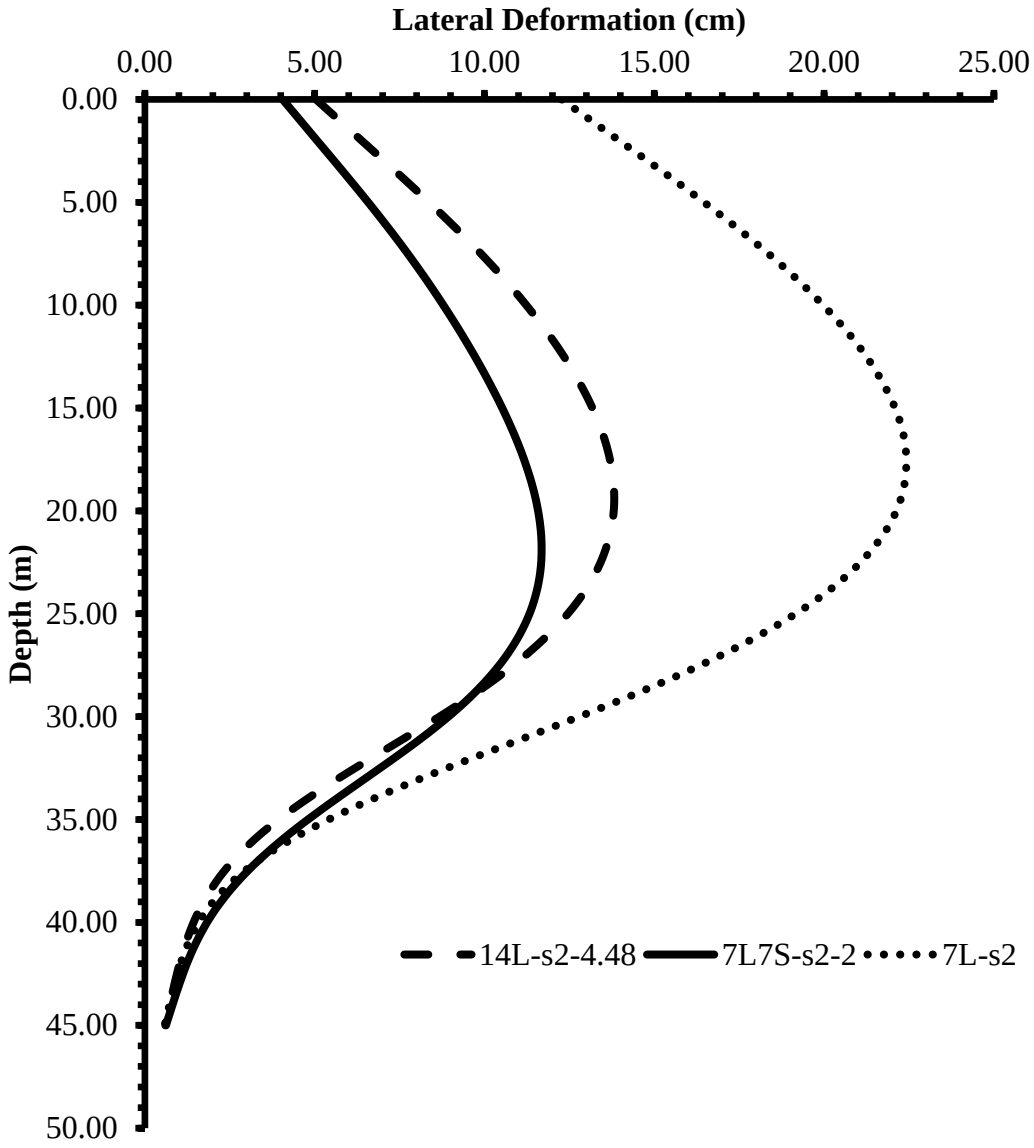

Figure 3.17. Comparison of Lateral Deformations for Equal Addition Models

3.2.3. Constant Horizontal Spacing Comparison

For this scenario, horizontal spacing of anchors is fixed at 2m while keeping other conditions same. Details of the constant horizontal spacing comparison models are presented below.

Table 3.13. Details of Constant Horizontal Spacing Comparison

Model Name	Total Anchor Quantity	Anchor Length per Meter
7L-s2	293m (7L) / 2m	146.5 m/m
7L7S-s2	293m (7L) / 2m + 126m (7S) / 2m	209.5 m/m
14L-s2	293m (7L) / 2m+ 282 (7L) / 2m	287.5 m/m

Results of constant horizontal spacing comparison are presented below.

Table 3.14. Results of Constant Horizontal Spacing Comparison

Model Name	Max. Lateral Deformation (cm)	Factor of Safety
7L-s2	22.42	1.291
7L7S-s2	11.68	1.373
14L-s2	8.86	1.560*

*Due to high density of anchors, failure surface is shifted outside the bond lengths.

Results show that with less anchor, 7L7S model decreases deformations significantly with less anchor quantity. Also, slight increase in the factor of safety is also observed in this model too.

To compare the efficiency of each model, an efficiency parameter for anchored retaining wall (η) is derived. It should be noted that higher the efficiency, more efficient the design is.

$$\eta = \frac{\min\{FS, FS_{limit}\}}{\max\left\{\left(\frac{\delta}{H}\right), \left(\frac{\delta}{H}\right)_{limit}\right\} \cdot Q_{anchor} \cdot t_{wall}^{tc} \cdot ED_{wall}^{ec}} \quad (12)$$

In this formula, FS: Factor of safety of the design, FS_{limit}: Minimum factor of safety allowed, δ/H: Maximum lateral deformation normalized with excavation depth (m/m), $(\delta/H)_{limit}$: Maximum lateral deformation normalized with excavation depth allowed, Q_{anchor}: Anchor quantity per meter, t_{wall}: Thickness of the wall, tc: Thickness coefficient, ED_{wall}: Embedment depth of the wall, ec: Embedment coefficient. Higher efficiency coefficient means more efficient design. Thickness and embedment coefficients should be determined based on the comparison of costs and constructability. Efficiency formulation assumes that any more improvement beyond limits is over-design, thus should have no effect on the efficiency. Additional parameters can be adopted such as FS against basal heave. Also, efficiency parameter can be separated such as serviceability efficiency by neglecting FS parameter or ultimate limit state efficiency by neglecting deformation parameter (assuming that deformations are below ultimate state levels). For comparison purposes, FS_{limit}=1.3-1.5 and $(\delta/H)_{limit}$=0.002-0.003 will be adopted in this study. Since diaphragm wall design is same for all models, wall parameters in the efficiency formula are neglected.

Table 3.15. Comparison of Efficiencies of Each Model – Most efficient model is written in bold.

Scenario	**Model Name**	**Efficiency for FS_{limit}=1.5 $(\delta/H)_{limit}$=0.002**	**Efficiency for FS_{limit}=1.3 $(\delta/H)_{limit}$=0.003**
Equal Anchor Quantity	7L-s2	1.1792	1.1792
	7L7S-s2.86	**1.6200**	**1.5979**
	14L-s3.93	1.2000	1.2000
Equal Addition to 7L Model	7L-s2	1.1792	1.1792
	7L7S-s2-2	**1.6833**	**1.5938**
	14L-s2-4.48	1.5225	1.3474
Constant Horizontal Spacing	7L-s2	1.1792	1.1792
	7L7S-s2	1.6833	**1.5938**
	14L-s2	**1.7666**	1.5072

3.2.4. Effect of Single Anchor

Effect of each anchor on the behavior of retaining wall is also investigated. To compare the single anchor effect, 8L and 7L1S models are created. These models add only one long and short anchor to 7L model, respectively. Location of additional anchor is varied to observe the effect of each anchor. As expected, due to belly shape of the retaining wall deformations, 4th and 5th level anchors are the most effective when deformations are the main concern.

Comparison of factors of safety for each anchor yields interesting results. As previously described, increase in factor of safety due to short anchors is also related to shear bands formed between failure surface and wall. Based on the comparisons of factors of safety for each addition of short anchor (1st short anchor level is located at -4.00m and 7th is located at -28.00m) it is observed that the 1st short anchor is mostly responsible for the increase in the factor of safety. Results also show that effect of short anchors on the factor of safety are not cumulative, since small shear bands require fewer anchors to be improved due to lower driving forces. Increase in factor of safety for 7L7S model mainly depends on the upper level anchors.

Comparisons of deformation and factor of safety for each additional short and long anchor are given in *Figure 3.18* to *Figure 3.21*. Vertical axis in the figures shows the location of one additional short anchor. It should be noticed that the graphs in these figures are not displacement profiles but each one of the points are additional analyses with different location of additional single anchor.

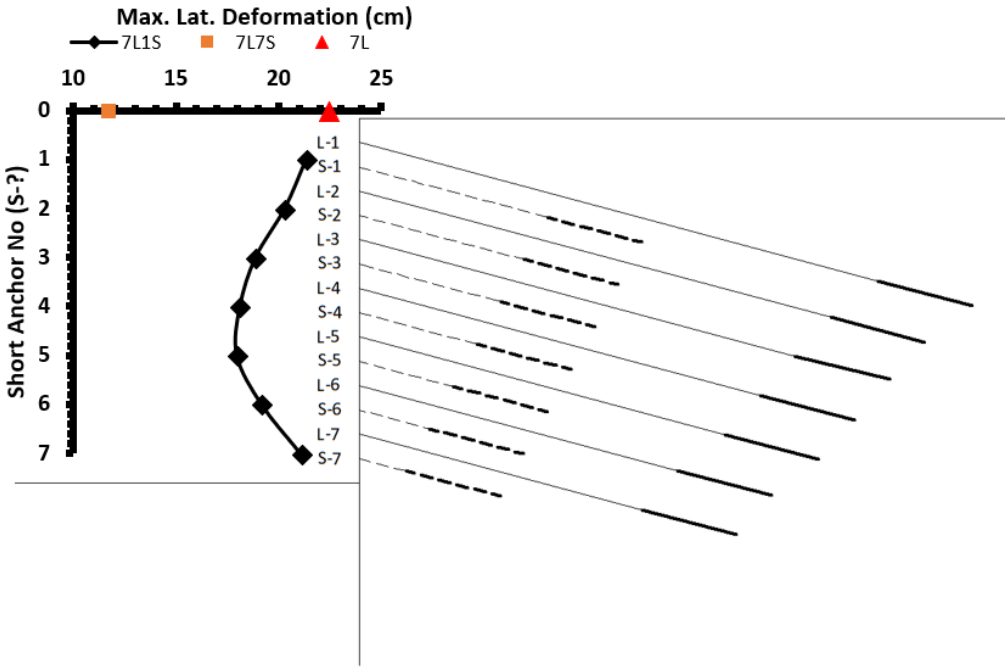

Figure 3.18. Effect of Each Short Anchor on the Max. Lat. Deformation (7L1S)

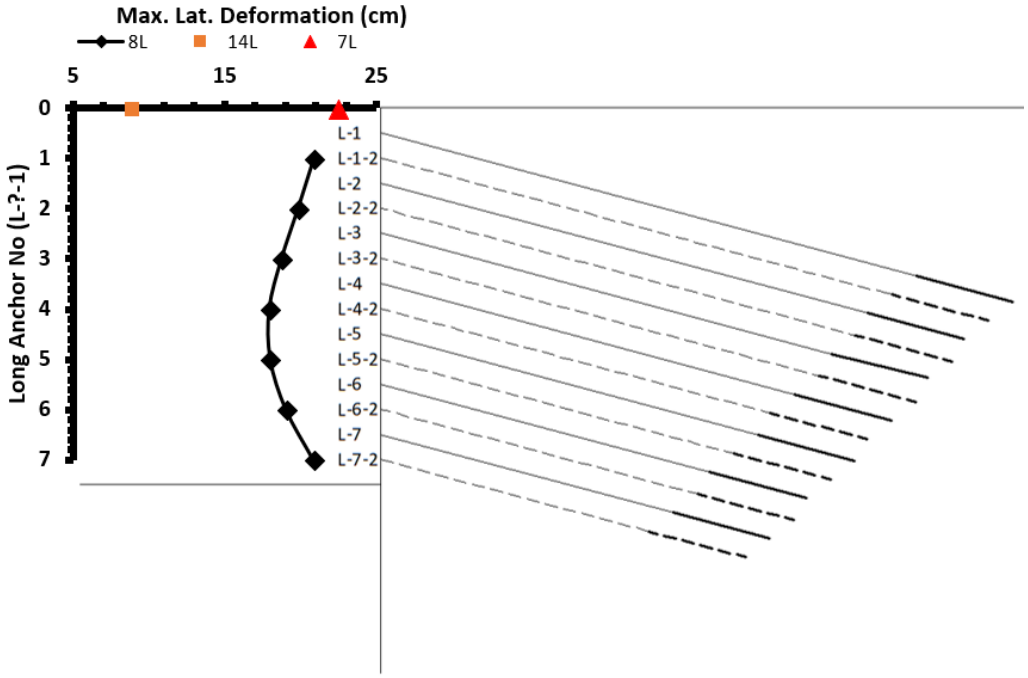

Figure 3.19. Effect of Each Long Anchor on the Max. Lat. Deformation (8L)

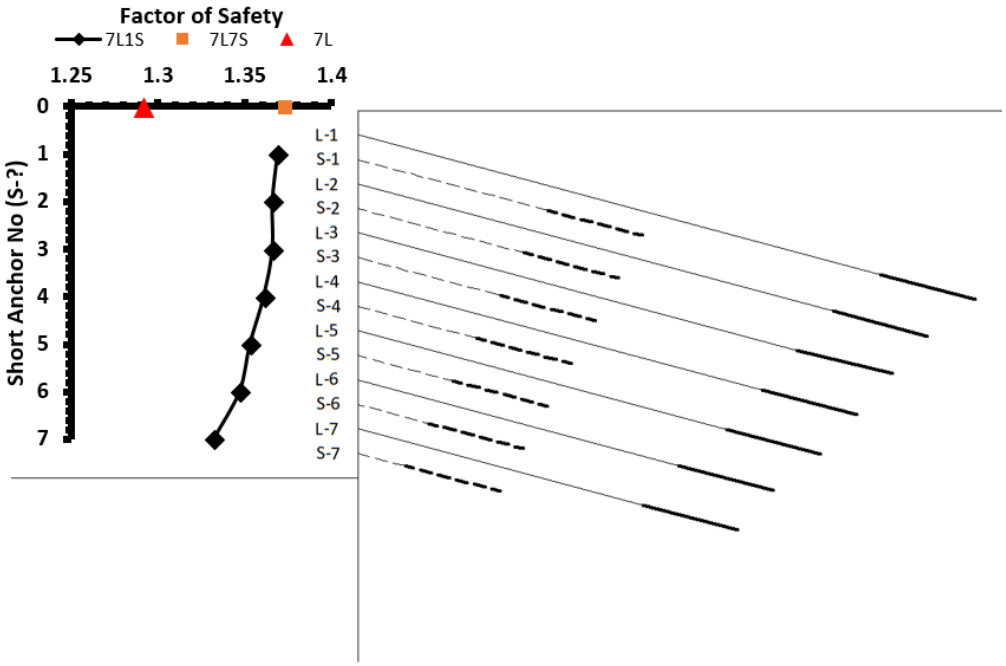

Figure 3.20. Effect of Each Short Anchor on the Factor of Safety (7L1S)

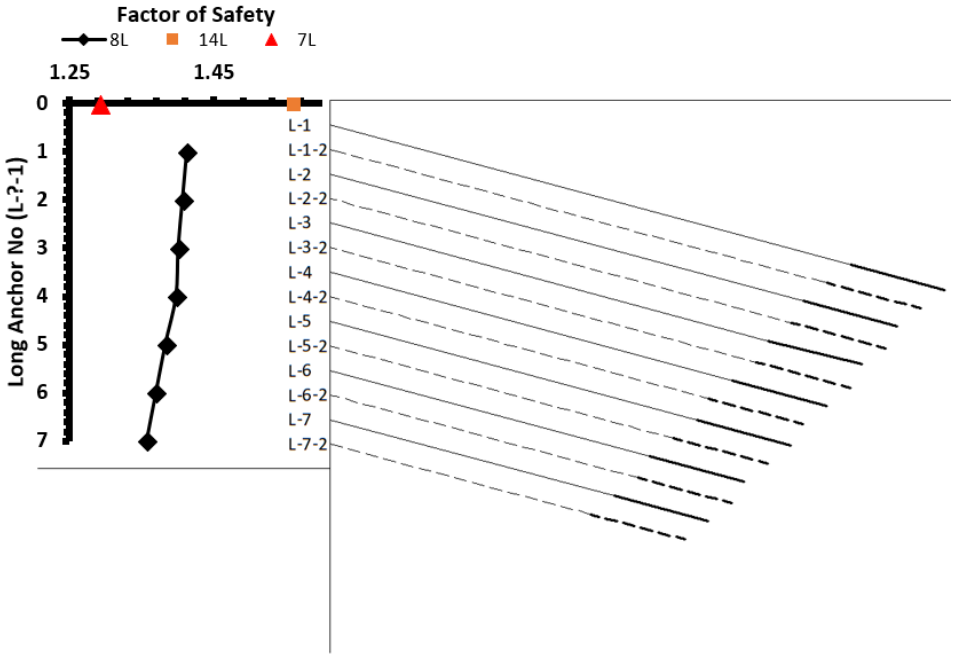

Figure 3.21. Effect of Each Long Anchor on the Factor of Safety (8L)

Incremental deviatoric strains of 7L1S-1 and 7L1S-7 are presented below. Figure shows that short anchor at 1st level improves more shear bands than the one located at the 7th.

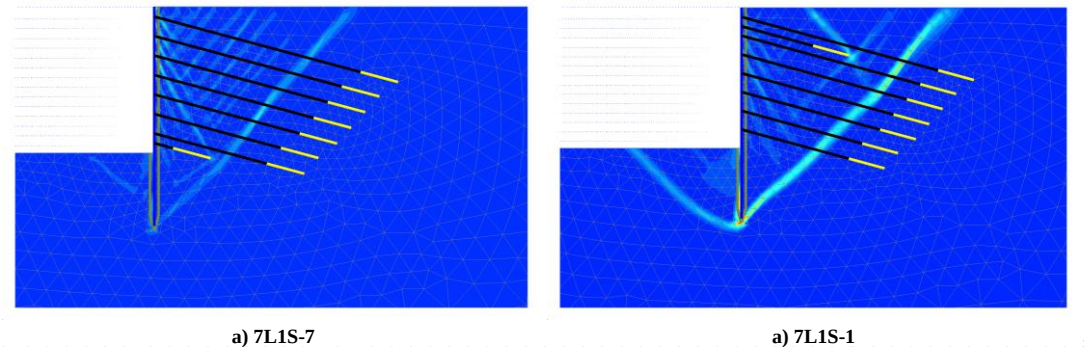

a) 7L1S-7 a) 7L1S-1

Figure 3.22. Comparison of Shear Bands of a) 7L1S-7 and b) 7L1S-1 Models

3.2.5. Effect of Software and Soil Models

To double check the result and avoid software-based errors, Optum G2 (Krabbenhoft & Lyamin, 2014) finite element package is used and compared with Plaxis results. 6-node gauss elements with mesh adaptivity options are used In Optum calculations. Optum G2 is a finite element limit analysis tool developed by Optum CE of Denmark. G2 can perform limit analysis on finite element models, such as calculating upper and lower limit bound capacity of a shallow foundation, slope etc. Advanced mesh adaptivity tool is also very convenient for safety analyses since failure surface is not predetermined and additional mesh refinement around high strain surfaces may provide better estimation of FS.

Table 3.16. Comparison of Plaxis and Optum G2 with Constant Horizontal Spacing Comparison Models

FE Package	Plaxis	Optum G2
7L – FS	1.291	1.303
7L – Max. Lat. Def. (cm)	22.42	21.29
7L7S – FS	1.373	1.380
7L7S – Max. Lat. Def. (cm)	11.68	11.23
14L – FS	1.560	1.578
14L – Max. Lat. Def. (cm)	8.86	8.14

Results are quite similar to each other; therefore, it can be concluded that calculated results are not software dependent and can be reproduced using any finite element package with given assumptions. Failure surface for 7L7S-s2 model in Optum G2 is shown in Figure 3.23.

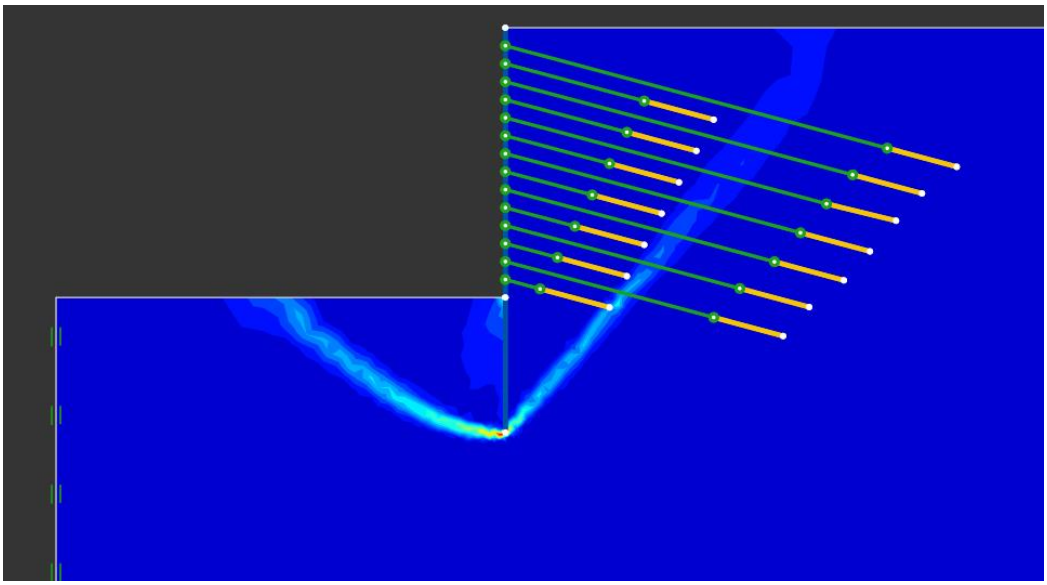

Figure 3.23. Failure Surface of 7L7S-s2 Model in Optum G2

Lastly, to investigate the effect of soil model, Hardening Soil with Small Strain Stiffness Model (HSSmall) is used and compared with HS Model results. HSSmall

model parameters are calculated as follows: PI is assumed 20 and using Vucetic and Dobry's (1991) curves reference strain is calculated as 2.85 x 10^{-4}. Using Alpan's (1970) chart and elastic theory with reloading poisson ratio as 0.2, maximum shear modulus is calculated as 162 MPa.

Due to similar strength modeling of HS and HSSmall, safety factor does not differ significantly. Comparison of lateral deformations are presented below. Conclusions drawn for short anchors using HS model are valid for HSSmall model too.

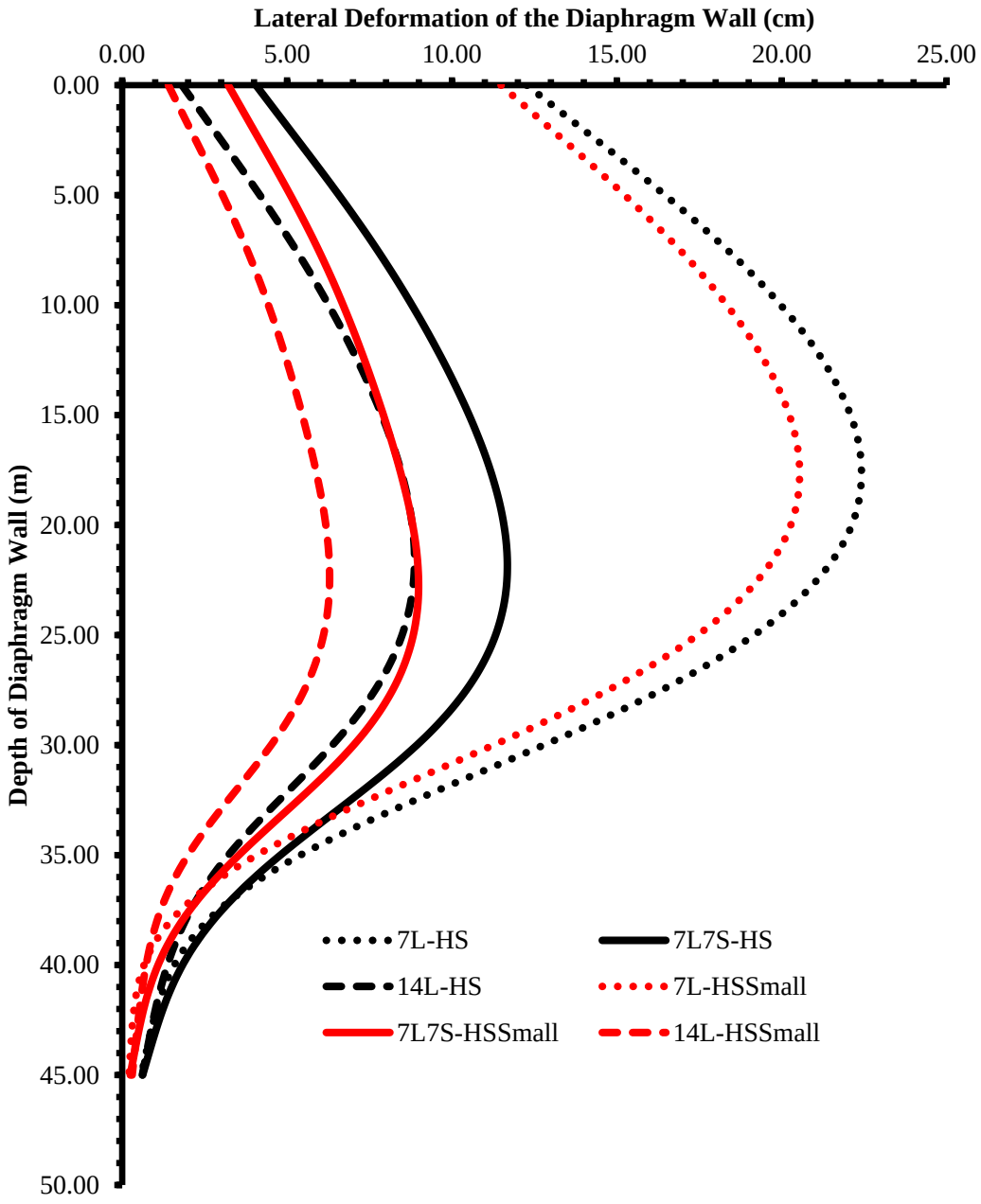

Figure 3.24. Comparison of HSSmall and HS Models for Constant Horizontal Spacing Case

Similar calculations are performed using Soft Soil model as well. Model parameters are calculated using the oedometric modulus and unloading/reloading modulus which are also adopted in HS and HSSmall models. Results of deformation analyses are presented in tabular form for comparison.

Table 3.17. Comparison of Different Soil Models for Constant Horizontal Spacing

Model Name	**Maximum Lateral Deformation (cm)**		
	HS	**HSSmall**	**Soft Soil**
7L-s2	22.42	20.55	19.14
7L7S-s2	11.68	8.98	6.05
14L-s2	8.86	6.29	4.66

Results clearly indicate that significant performance of short anchors on the deformation behavior of the retaining wall is not constitutive model dependent. Although calculated deformations differ significantly for different soil models, conclusions that are drawn using HS model are still valid for HSSmall and Soft Soil models. Due to implemented Mohr-Coulomb failure criteria in all soil models, safety factors do not differ significantly.

3.3. Effect of Association on the Failure Surface

Effect of dilatancy angle, therefore degree of non-associativity (ϕ-ψ), on the failure surface and oscillation behavior of the safety factor have been investigated in this chapter.

Comparisons have been performed for 7L7S-s2 model with different dilatancy angles. Figure 3.25 shows failure surfaces interpreted from total deviatoric strains.

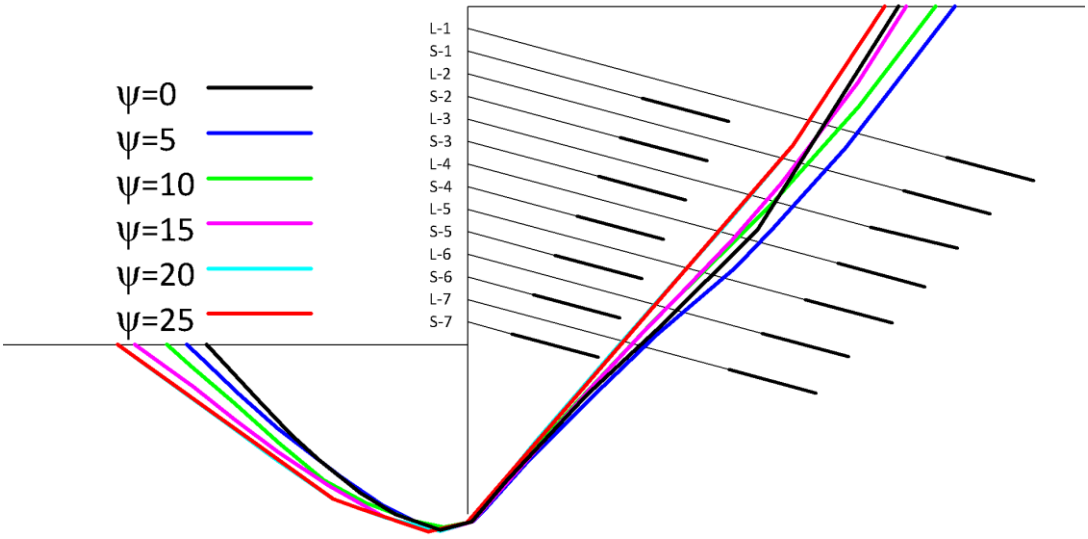

Figure 3.25. Comparison of Failure Surfaces for Different Dilatancy Angles (ϕ=25°)

Results show the range of failure surfaces obtained for 7L7S model. For dilatancy angles 20° and 25°, failure surfaces coincide. Inclinations are measured at various depths and found that for anchored retaining walls, simple characteristics are found to be not enough to describe the behavior. To compare stress characteristics (45+ϕ/2) and velocity characteristics (45+ψ/2), another term named "failure angle, λ" is defined. This angle describes the inclination of the failure surface as 45+λ/2° from the horizontal for active side and as 45-λ/2° for the passive side.

For passive side, non-associated material with ψ=0° fails with λ=4°. Failure angle increases with degree of non-associativity up to 18°. For smaller dilatancy angles (ψ<20), passive failure angle lies in the range of ϕ>λ>ψ, however, as degree of non-associativity (ψ-ϕ) decreases passive failure angle is limited at 18°.

For the active side, three-fold failure surface that can be defined with three failure angles is observed. Failure angles approach to stress characteristics between 1st anchor and ground level and becomes less dependent on the dilatancy angle. However, in other parts, failure angles differ from the defined range by stress and velocity characteristics with even negative failure angles. Therefore, it is crucial to perform

detailed nonlinear finite element analyses to investigate overall stability behavior rather than simple methods like limit equilibrium or beam on springs approach (Winkler, 1867) for anchored retaining walls.

Inclinations of failure surfaces for $\psi=0°$ and $\psi=25°$ cases are given below.

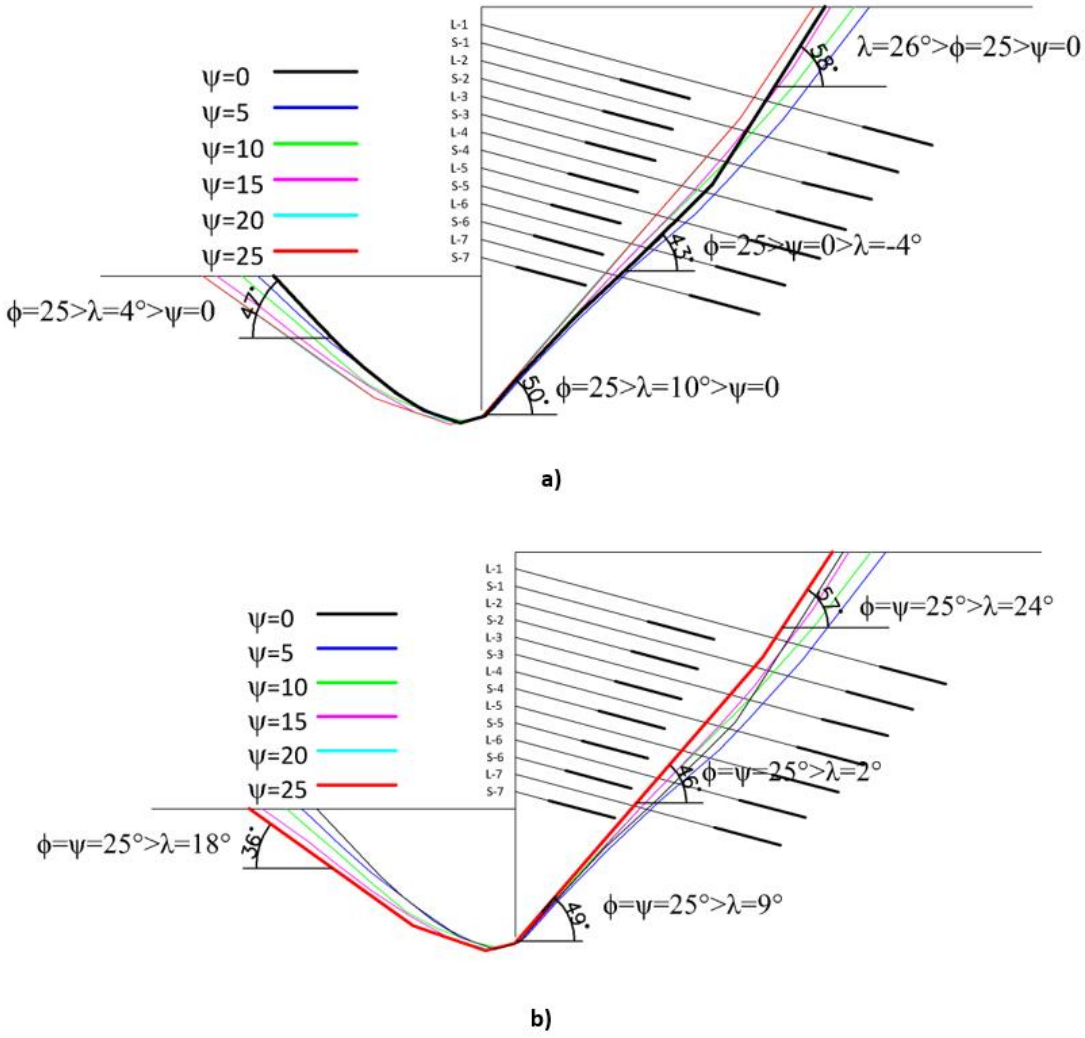

Figure 3.26. Detailed Representation of a) Non-associated case (ψ=0°) and b) of a) Associated case (ψ=25°)

Another important observation is on the oscillation behavior. Slope problems like Tschuchnigg et. al. (2015) is not kinematically constrained. However, cases such as anchored retaining wall are relatively more constrained. Tschuchnigg et. al. (2015) observed that for associated flow, oscillation is very small while for non-associated materials oscillation is more pronounced. Also, more importantly, for associated material behavior solution is unique, while for non-associated materials oscillation is due to varying failure surfaces. Independent review of the problem shows that oscillation of associated material is in order of 5 x 10-3 and standard deviation is 2.532 x 10-3. Although this value is very small and hard to observe in a graph, this oscillation is constant from earlier steps. *Figure 3.27* shows the reproduced associated case FS vs. step number graph. Constant oscillation can be seen in the close-up view.

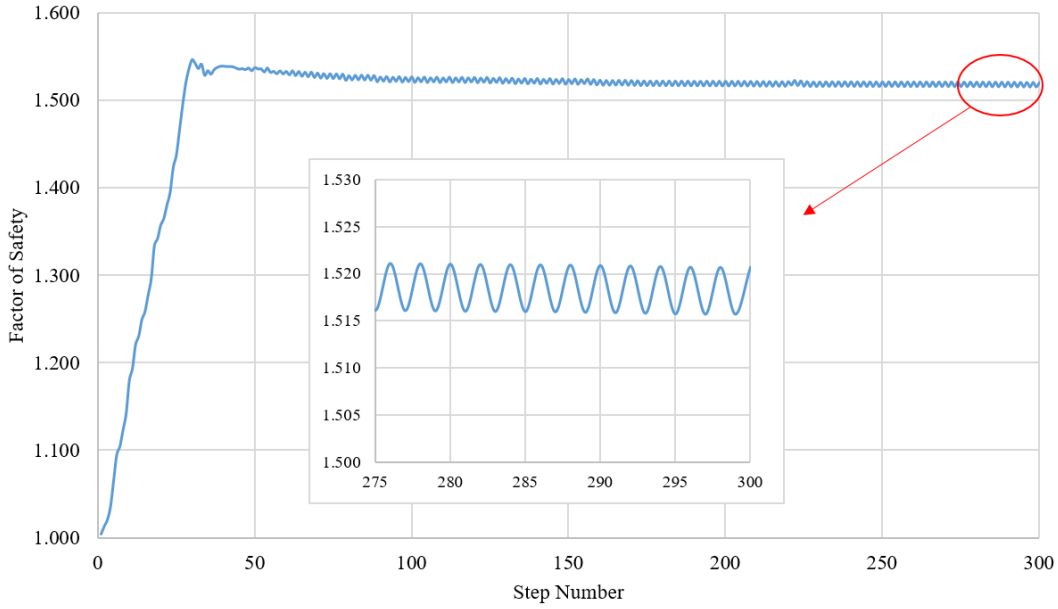

Figure 3.27. Tschuchnigg et. al. (2015) Associated Case Reproduced – FS vs. Step Number

Investigation of oscillation in all three models with constant horizontal spacing (s_h=2m) is given below. Interestingly, highest factor of safety is obtained with dilatancy angle 15° for 7L7S model. For other models, dilatancy angles between 15°-25° result in almost same and highest factor of safety. Results show that for a

kinematically constrained anchored retaining wall problem, widely known assumption of higher strength with increasing dilatancy (Vermeer & De Borst, 1984) does not hold true for every case.

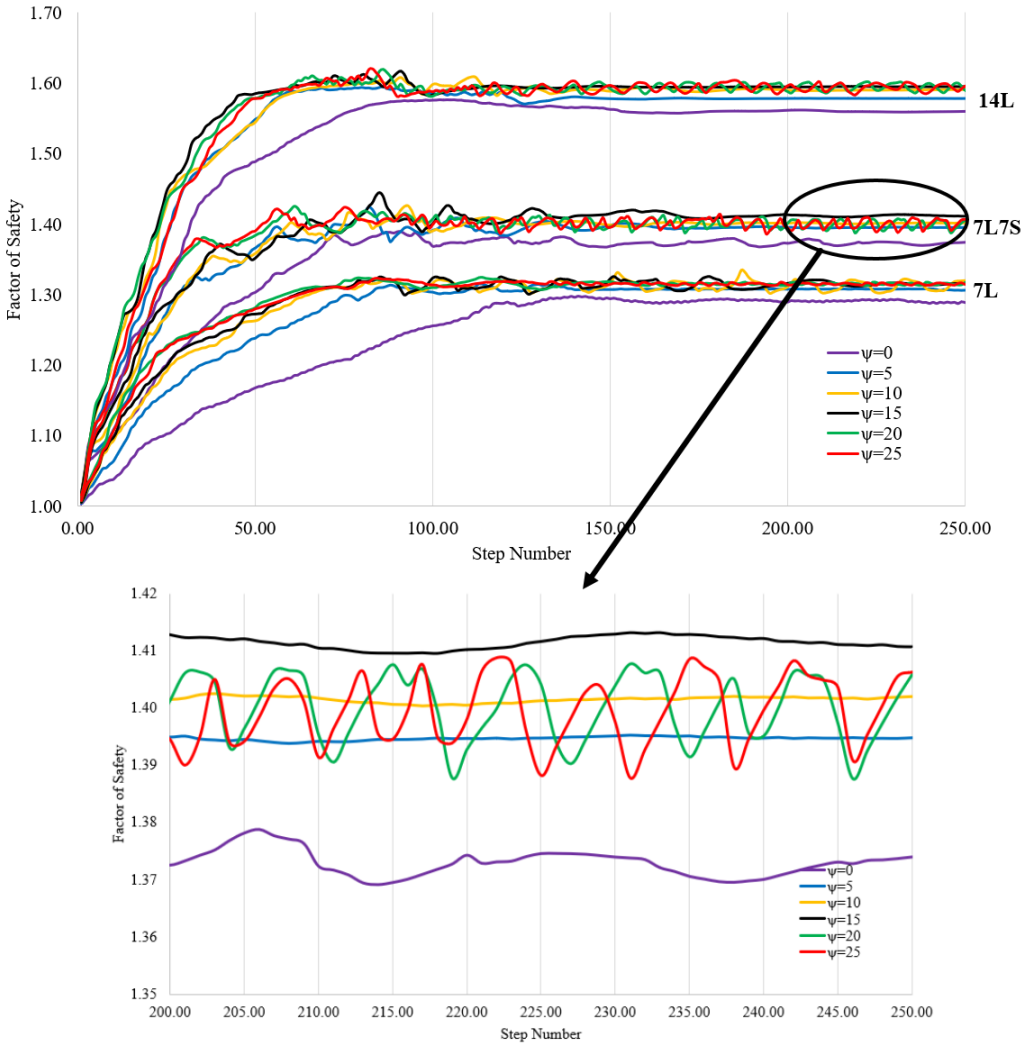

Figure 3.28. Oscillation Behavior of Factor of Safety with Safety Analysis Steps

Oscillations are compared by standard deviation of last 50 steps vs. dilatancy angle below. As can be seen, most oscillating dilatancy angle is not constant for all models. Contrary to previous findings on kinematically unconstrained problem by Tschuchnigg et. al. (2015), associated case definitely not has a steady safety factor. Also, as the problem is kinematically constrained, varying failure surfaces are not observed for non-associated cases. As Potts and Zdravkovic (2001) states, for kinematically constrained cases, change in the location of rupture surface is restricted, therefore change in the strength of rupture surface occurs. Therefore, smaller freedom to form new failure surfaces and shear bands may result in different oscillation behavior. Non-uniqueness of the solution may not present itself for kinematically constrained solutions.

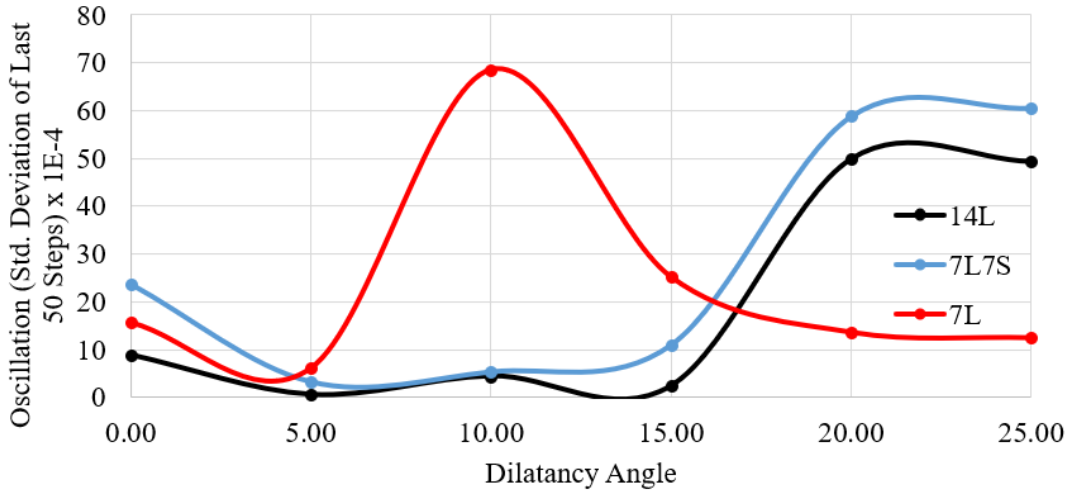

Figure 3.29. Comparison of Oscillation with Standard Deviation for Different Dilatancy Angles

CHAPTER 4

SUMMARY, CONCLUSION AND FUTURE WORK

4.1. Summary

This study investigates performance of short anchors in retaining walls and comparison with long anchors. Short anchors are defined as the anchors of which bond lengths are placed inside the failure wedge. Using short anchors are prohibited in almost all international standards.

Firstly, with the correct assumptions made, effect of anchor modeling on the retaining wall behavior is investigated. Then, performance of short anchors is investigated using different scenarios:

- Equal Anchor Quantity
- Equal Addition to Base Model
- Constant Horizontal Spacing

Analyses were carried out using, mainly, Plaxis 2D Finite Element Package with additional analysis using Optum G2 and Plaxis 3D. Results are presented throughout the text to compare short and long anchor performance.

Lastly, since this study deals with deformation and safety factor comparison of different cases, effects of association on the failure surface have been investigated. Since associativity strongly affects the failure surface and load-displacement behavior, analyses have been included as well.

4.2. Conclusion

The outcomes and conclusions of this study are listed as the followings:

- To obtain correct failure surface and safety factor, anchor modeling is crucial. Elastic anchor models, due to infinite loading of the strands and bond length, shift the failure surface to the outside of anchored zone. However, in reality, anchors fail after a certain amount of tensile load which depends on the strength of strands or grout/ground interface.
- The difference between failure surface shape and safety factor using elastic and elasto-plastic anchor models are significant.
- Equal Anchor Quantity comparisons have shown that 7L7S model which uses short anchors combined with long anchors are most effective to reduce deformations. Results show that maximum lateral deformation of 7L7S model is 25% less than other models that only use long anchors. Also, safety factor comparisons have shown that, 7L7S model's FS is slightly higher than other models that implement long anchors. The reason behind this difference is due to 25% difference in the deformations. Due to equal anchor quantity scheme, densely spaced short anchors reduce the load on the long anchors, therefore delays the failure of long anchors before mobilization of failure surface. Also, shear bands between failure surface and wall are prevented using short anchors which eventually strengthen the failure wedge. To validate 2D procedure and check the results, 3D analyses were performed for equal anchor quantity comparison models. Results matched with 2D analyses except that 7L7S model's factor of safety is higher in 3D analysis.
- Second comparison scheme is created assuming equal addition to 7L model. To the base model 7L-s2, short and long anchors are added. Quantity of addition to 7L model is kept same in order to compare the short and long anchors with respect to practical purposes. Results have show that short anchors decrease the deformation of 7L model by 48% while long anchors decrease it by 38%. Therefore, it can be concluded that short anchors are 25%

more efficient than long anchors in deformation control. Addition of short anchors to 7L model does not cause any problem, instead increase the safety factor by a small amount.

- Lastly, constant horizontal spacing comparisons are performed. Horizontal spacing is kept constant at 2m. Results show that 7L7S model decreases the deformations significantly with less anchor compared to 14L model. Comparison of efficiencies showed that 7L7S model is superior to others in almost all cases.
- To investigate the effect of each anchor on the performance of system, 8L and 7L1S models are created. Position of additional one anchor to 7L model is varied in analyses. The interesting result is obtained for comparison of safety factor of 7L1S and 7L7S models. Results have shown that upper level short anchors, due to their position relative to shear bands, improve the safety factor to the level of 7L7S model. Therefore, it can be concluded that small increase in the safety factor of 7L7S model mainly depends on the upper level anchors due to improvement in shear bands.
- Efficiency of each design is calculated using a procedure developed in this study, called "efficiency coefficient."
- To avoid software-based errors, Optum G2 was used for validation. Results were found to be very similar and not software-dependent. Results were also validated using HS-Small and Soft Soil models.
- In the last section, effect of association is investigated. 7L7S-s2 models with different dilatancy angles are analyzed. Failure surface variation based on the dilatancy angle shows that anchored retaining walls cannot be modeled using simple hand calculation rules. Failure surface orientation varies to negative failure angle values in some parts and gets closer to Rankine failure surface in un-anchored zone between ground level and 1st level anchor.
- Also, oscillation behavior of the safety factor vs. step is discussed in the text. Results are compared with results of Tschuchnigg et. al. (2015) and contrary

to their findings, oscillation behavior does not reduce with increasing dilatancy angle for anchored retaining walls. Also, it is not possible to agree with common finding that strength increases with increasing dilatancy for anchored retaining wall case. Results have shown that behavior is highly erratic and may change with different models.

To sum up the results, in this thesis, it is proven within the capabilities of finite element analyses and constitutive models used in the analyses, if overall stability is ensured by long anchors, to reduce lateral deformations, short anchors can be used and have no harmful effect on the retaining wall behavior. Internationally accepted standards should not completely ban or discourage short anchors, but instead should define a requirement for long anchors to provide overall stability only. If overall stability in ensured using long anchors, lateral deformations and hence, ground settlements can be reduced using short anchors.

4.3. Future Work

Followings are recommended for future works that investigate performance of short anchors:

- Complete 3D comparison of performance of short and long anchors.
- Scaled model tests and full-scale field tests can be performed.
- Optimization of real cases with short anchors needs to be included for field validations.

REFERENCES

Alpan, I. (1970). The geotechnical properties of soils. *Earth-Science Reviews*, *6*(1), 5–49.

Anderson, W. F., Hanna, T. H., & Abdel-Malek, M. N. (1983). Overall stability of anchored retaining walls. *Journal of Geotechnical Engineering*, *109*(11), 1416–1433.

ASTM. (2017). *Standard Specification for Low-Relaxation, Seven-Wire Steel Strand for Prestressed Concrete*.

Atkinson, J. H., & Sallfors, G. (1991). Experimental determination of stressstrain-time charactristics in laboratory and in situ tests. *Proceedings, 10th ECSMFE, Florence, Rotterdam: Balkema*, 959–999.

Benz, T. (2007). *Small-strain stiffness of soils and its numerical consequences*. Univ. Stuttgart.

Benz, T., Schwab, R., & Vermeer, P. (2009). Small-strain stiffness in geotechnical analyses. *Bautechnik*, *86*(S1), 16–27.

Bolton, M. D., & Powrie, W. (1988). Behaviour of diaphragm walls in clay prior to collapse. *Géotechnique*, *38*(2), 167–189.

Bransby, P. L. (1968). *Stress and strain in sand caused by rotation of a model wall*. University of Cambridge.

Bransby, P. L., & Milligan, G. W. E. (1975). Soil deformations near cantilever sheet pile walls. *Geotechnique*, *25*(2), 175–195.

Briaud, J.-L., & Lim, Y. (1999). Tieback walls in sand: numerical simulation and design implications. *Journal of Geotechnical and Geoenvironmental Engineering*, *125*(2), 101–110.

Brinkgreve, R B J, Kappert, M. H., & Bonnier, P. G. (2007). Hysteretic damping in a small-strain stiffness model. *Proc. of Num. Mod. in Geomech., NUMOG X, Rhodes*, 737–742.

Brinkgreve, Ronald B J. (2005). Selection of soil models and parameters for geotechnical engineering application. In *Soil constitutive models: Evaluation, selection, and calibration* (pp. 69–98).

British Standards Institution. (2004). *BS EN 1997 - Eurocode 7 - Geotechnical design, Part 1*.

British Standards Institution. (2015). *BS 8081 - Code of practice for grouted anchors*.

Britto, A. M., & Gunn, M. J. (1987). *Critical state soil mechanics via finite elements*.

Broms, B. B. (1968). Swedish Tie-Back Systems for Sheet Pile Walls. *Acta Technica*.

Broms, B. B. (1988). Design and construction of anchored and strutted sheet pile walls in soft clay. In *Second International Conference on Case Histories in Geotechnical Engineering*.

Canadian Geotechnical Society. (2006). *Canadian foundation engineering manual* (4th ed.). Canadian geotechnical society.

Chen, W.-F. (1975). *Limit Analysis and Soil Plasticity*. Elsevier.

Chen, W.-F., & Liu, X. L. (2012). *Limit analysis in soil mechanics* (Vol. 52). Elsevier.

Cheng, Y., Wong, H., Leo, C. J., & Lau, C. K. (2016). *Stability of Geotechnical Structures: Theoretical and Numerical Analysis*. Bentham Science Publishers.

Chowdhury, R., Flentje, P., & Bhattacharya, G. (2009). *Geotechnical slope analysis*. Crc Press.

Clayton, C. R. I., Woods, R. I., Bond, A. J., & Milititsky, J. (2014). *Earth pressure and earth-retaining structures*. CRC Press.

Coulomb, C. A. (1773). Essai sur une application des règles de maximis et minimis à quelques problèmes de statique relatifs à l'architecture. *Mem. Div. Sav. Acad.*, 7.

Davis, E. H. (1968). Theories of plasticity and failures of soil masses. *Soil Mechanics, Selected Topics*.

Do, T.-N., Ou, C.-Y., & Chen, R.-P. (2016). A study of failure mechanisms of deep excavations in soft clay using the finite element method. *Computers and Geotechnics*, *73*, 153–163.

Duncan, J. M., & Chang, C.-Y. (1970). Nonlinear analysis of stress and strain in soils. *Journal of Soil Mechanics & Foundations Div*.

Duncan, J. M., Wright, S., & Brandon, T. (2014). *Soils Strenght and Slope Stability*. *Soil Strength and Slope Stability*. John Wiley & Sons.

European Committee for Standardization. (2004). EN 1992-1-1 Eurocode 2: Design

of concrete structures - Part 1-1: General rules and rules for buildings. Brussels: CEN.

European Committee for Standardization. (2005). EN 10138-3 Prestressing Steel - Part 3: Strand. Brussels: CEN.

Gajo, A., Bigoni, D., & Wood, D. M. (2004). Multiple shear band development and related instabilities in granular materials. *Journal of the Mechanics and Physics of Solids*, *52*(12), 2683–2724.

Graham, J., Noonan, M. L., & Lew, K. V. (1983). Yield states and stress--strain relationships in a natural plastic clay. *Canadian Geotechnical Journal*, *20*(3), 502–516.

Hardin, B., & P. Drnevich, V. (1972). Shear Modulus and Damping in Soils: Design Equations and Curves. *J. Soil Mech. Found. Div.*, *98*.

Hong Kong Civil Engineering Department. (1996). *Pile design and construction*. CRC Press.

Juran, I., & Elias, V. (1991). Ground anchors and soil nails in retaining structures. In *Foundation engineering handbook* (pp. 868–905). Springer.

Kempfert, H.-G., & Gebreselassie, B. (2006). *Excavations and foundations in soft soils*. Springer Science & Business Media.

Kirkgard, M. M., & Lade, P. V. (1993). Anisotropic three-dimensional behavior of a normally consolidated clay. *Canadian Geotechnical Journal*, *30*(5), 848–858.

Krabbenhoft, K. (2018a). *OptumG2 Material Manual*. *Optum Computational Engineering*.

Krabbenhoft, K. (2018b). *OptumG2 Theory Manual*. *Optum Computational Engineering*.

Krabbenhoft, K., Karim, M. R., Lyamin, A. V, & Sloan, S. W. (2012). Associated computational plasticity schemes for nonassociated frictional materials. *International Journal for Numerical Methods in Engineering*, *90*(9), 1089–1117.

Krabbenhoft, K., & Lyamin, A. V. (2014). Optum G2. *Optum Computational Engineering*.

Kranz, E. (1953). Über die Verankerung von Spundwänden. *TU Lib 13768530 (000151256)*.

Kulhawy, F. H., & Mayne, P. W. (1990). *Manual on Estimating Soil Properties for Foundation Design*. *EPRI EL-6800*. https://doi.org/EPRI-EL-6800

Mair, R. J. (1993). Developments in Geotechnical Engineering Research: Application to Tunnels and Deep Excavations. In *Proceedings of the Institution of Civil Engineers-Civil Engineering* (Vol. 97, pp. 27–41).

NAVFAC. (1986). Foundations & Earth Structures. *Naval Facilities Engineering Command*, 279. https://doi.org/10.7498/aps.62.113201

Obrzud, R. F. (2010). On the use of the Hardening Soil Small Strain model in geotechnical practice. *Numerics in Geotechnics and Structures*, 15–32.

Ou, C.-Y. (2006). *Deep excavation: Theory and practice*. CRC Press.

Parry, R. H. G. (2014). *Mohr circles, stress paths and geotechnics*. CRC Press.

Plaxis BV. (2017a). *Plaxis 2D Material Models Manual*. Delft, Netherlands.

Plaxis BV. (2017b). *Plaxis 2D Reference Manual*. Delft, Netherlands.

Plaxis BV. (2017c). *Plaxis 3D 2016.2*. Delft, Netherlands.

Post-Tensioning Institute. (2004). *Recommendations for Prestressed Rock and Soil Anchors* (4th ed.). Post-Tensioning Institute.

Potts, D. M., Axelsson, K., Grande, L., Schweiger, H., & Long, M. (2002). *Guidelines for the use of advanced numerical analysis*. *Thomas Telford Ltd*. https://doi.org/10.1680/gftuoana.31258

Potts, D. M., & Zdravkovic, L. (2001). *Finite element analysis in geotechnical engineering*. *Thomas Telford Ltd* (Vol. 2).

Poulos, H. G., Carter, J. P., & Small, J. C. (2001). Foundations and retaining structures – research and practice. In *Proceedings International Conference on Soil Mechanics and Foundation Engineering* (p. 80 p.).

Poulos, Harry G. (2017). *Tall Building Foundation Design*. CRC Press.

Puller, M. (2003). *Deep excavations: A practical manual* (Second edi). Thomas Telford Publishing. https://doi.org/10.1680/deapm.34594

Rankine, W. J. M. (1857). On the Stability of Loose Earth. *Philosophical Transactions of the Royal Society of London*, *147*(0), 9–27. https://doi.org/10.1098/rstl.1857.0003

Roscoe, K. H. (1970). The influence of strains in soil mechanics. *Geotechnique*, *20*(2), 129–170.

Rowe, P. W. (1962). The stress-dilatancy relation for static equilibrium of an assembly of particles in contact. *Proc. R. Soc. Lond. A*, *269*(1339), 500–527.

Rowe, P. W., & Peaker, K. (1965). Passive Earth Pressure Measurements. *Géotechnique*, *15*(1), 57–78. https://doi.org/10.1680/geot.1965.15.1.57

Sabatini, P. J., Pass, D. G., & Bachus, R. C. (1999). *FHWA-IF-99-015 - GEC 04 - Ground Anchors and Anchored Systems*.

Santos, J. A., & Correia, A. G. (2001). Reference threshold shear strain of soil. Its application to obtain an unique strain-dependent shear modulus curve for soil. In *Proceedings of The International Conference on Soil Mechanics and Geotechnical Engineering* (Vol. 1, pp. 267–270). İstanbul, Turkey.

Schanz, T., Vermeer, A., & Bonnier, P. (1999). The hardening soil model: formulation and verification. *Beyond 2000 in Computational Geotechnics*, 281–296.

Seed, H B; Idriss, I. M. (1970). *Soil moduli and damping factors for dynamic response analysis*. *EERC 70-10*. Berkeley, California.

Sloan, S. W. (2013). Geotechnical stability analysis. *Géotechnique*, *63*(7), 531–571. https://doi.org/10.1680/geot.12.RL.001

Teo, P. L., & Wong, K. S. (2012). Application of the Hardening Soil model in deep excavation analysis. *IES Journal Part A: Civil and Structural Engineering*, *5*(3), 152–165. https://doi.org/10.1080/19373260.2012.696445

Terzaghi, K., Peck, R. B., & Mesri, G. (1996). *Soil Mechanics in Engineering Practice, Third Edition*. *Wiley-Interscience Publication, John Wiley and Sons, Inc.* https://doi.org/10.1016/S0013-7952(97)81919-9

Tschuchnigg, F., Schweiger, H. F., & Sloan, S. W. (2015). Slope stability analysis by means of finite element limit analysis and finite element strength reduction techniques. Part I: Numerical studies considering non-associated plasticity. *Computers and Geotechnics*, *70*, 169–177.

Vermeer, P. A., & De Borst, R. (1984). Non-associated plasticity for soils, concrete and rock. *HERON, 29 (3), 1984*.

Vucetic, M., & Dobry, R. (1991). Effect of soil plasticity on cyclic response. *Journal of Geotechnical Engineering*, *117*(1), 89–107.

Winkler, E. (1867). *Die Lehre von Elastizitat und Festigkeit (The theory of elasticity and stiffness). H. Domenicus*. Prague.

Xanthakos, P. P. (1991). *Ground anchors and anchored structures*. John Wiley & Sons.